DUPLICATE

METEOROLOGICAL OFFICE

Forecasting Research

FORECASTING RESEARCH DIVISION
TECHNICAL REPORT NO. 125

CAUSE AND CURE OF THE SUPERADIABATIC LAPSE RATE IN THE LIMITED AREA AND GLOBAL MODELS

by

C.A. WILSON, F. RAWLINS AND O.M. HAMMON

OCTOBER 1994

Meteorological Office
London Road
Bracknell
Berkshire
RG12 2SZ
United Kingdom

ORGS UKMO F
National Meteorological Library
FitzRoy Road, Exeter, Devon. EX1 3PB

FORECASTING RESEARCH TECHNICAL REPORT NO.125

CAUSE AND CURE OF THE SUPERADIABATIC LAPSE RATE IN THE LIMITED AREA AND GLOBAL MODELS

by

C.A.WILSON, F.RAWLINS and O.M.HAMMON

OCTOBER 1994

© CROWN COPYRIGHT 1994

Forecasting Research Division
Meteorological Office
London Road
Bracknell
Berks
RG12 2SZ

This Technical report has not been published. Permission to quote it must be obtained from the Head of Numerical Modelling, Forecasting Research Division.

CAUSE AND CURE OF THE SUPERADIABAT PROBLEM IN THE LIMITED AREA AND GLOBAL MODELS.

1. INTRODUCTION.

During January 1994, forecasters in CFO noted that the limited area model was producing occasional unrealistic forecast ascents in cold air outbreaks over the sea, with superadiabatic lapse rates above 800 hPa. Initially the cause was linked to the prior introduction of calling the convection every other timestep or to the convective downdraught scheme. A similar problem was noticed in the global model following the introduction of the frozen physics package on January 11th.

This note examines the causes of the superadiabatic lapse rate and assesses methods of curing the problem. The layout of this note is as follows:

Section 2	causes of the superadiabatic lapse rate
Section 3	four modifications to the boundary layer and convection are described and tested.
Section 4	limited area model tests on summer convection
Section 5	global model tests on trial week 7/1/94 - 13/1/94
Section 6	(a) objective verification scores for limited area model trials
Section 6	(b) objective verification scores for global model trials
Section 7	conclusions.

2. CAUSES OF THE SUPERADIABATIC PROBLEM.

The problem is illustrated by the T+12 limited area model forecast verifying at 18Z 5/1/94. Figure 1a shows a very cold unstable airmass in the eastern Atlantic circulating around a depression centred over Northern Ireland and Scotland. The area of interest, 46-50 degrees north, 10-20 degrees west, is enclosed within the >50% snow probability area. Within this area, the model was predicting both dynamic and convective precipitation. The ascent at 47N 14W, shown in Figure 1b, shows a superadiabatic lapse rate between 780 and 700 hPa. The lowest levels are very moist, producing low cloud and there is an apparent 'warm nose' at the top of the boundary layer. Further examples of superadiabatic lapse rates in both the global and limited area models occurred last winter in very cold air outbreaks over a relatively warm sea, (sea surface temperature 8-10C).

Two changes to the limited area model were made during 1993. The convective downdraught and rapidly mixing boundary layer schemes were introduced on the 27th April to improve the prediction of showers and a further upgrading of the physics was added on 7th December. On the latter date, a further change was made to call the convection on every other timestep.

In order to find the cause of the super-adiabatic lapse rate, the forecast shown in Figure 1 was rerun several times, taking out each element of the 1993 changes in turn. Ascents from four of these reruns are shown in Figure 2. The two main suspects initially were the change to the convective timestep and the convective downdraught scheme, but the

ascents shown in Figures 2a and 2b show that these two changes were innocent. When we reran our test case omitting each of these changes in turn, the superadiabatic lapse rate was still present. The model ascents at 47N 14W for these reruns are shown in Figure 2a (convection called every timestep) and Figure 2b (convective downdraught omitted). These two ascents are almost identical to the operational ascent, Figure 1b, apart from some low level humidity changes. Most of the other changes also had a null impact. However,the biggest impact on the superadiabatic lapse rate was obtained by omitting the rapidly mixing boundary layer. The ascent at 47N 14W for this rerun, shown in Figure 2c, shows no sign of the superadiabatic lapse rate and the boundary layer is much drier. A smaller impact was found by omitting the fully divergent ice scheme. The comparable ascent from this rerun, Figure 2d, is warmer between 750mb and 650mb, although there is still a superadiabatic lapse rate present.

Our tests show that the main cause of the superadiabatic lapse rate was the interaction between the non-local mixing of heat and moisture in the boundary layer and the convection scheme. Too much mixing done by the boundary layer removed most of the convective instability in the lower layers and suppressed convection. Very weak convection from the lower layers meant insufficient convective heating at 700 hPa. The flux divergent ice fallout also exacerbated the problem.

Without the rapidly mixing boundary layer, the convection scheme shuts off boundary layer mixing of all variables in all unstable situations. It does this by very efficiently removing all instability so the Richardson numbers seen by the boundary layer scheme are all neutral or even slightly stable. In the extreme cases, as illustrated by the superadiabat problem, convection does in fact dominate but in less extreme conditions better results are obtained by allowing boundary layer turbulent mixing to have a chance of operating. If boundary layer mixing is shut off everywhere the convection scheme will try to represent Sc but it will not do it properly because it's "split final detrainment" greatly overdoes the cloud top entrainment.

3. MODIFICATIONS TO CURE THE SUPER-ADIABATIC LAPSE RATE.

Four possible modifications to cure the problem are described below.

Mod "A"

This is a change to fallout of frozen precipitation in the large-scale precipitation scheme. The current operational scheme adds the ice fallout from any layer into the cloud water of the layer below. This can lead to rapid and unrealistic lowering of cloud base, sometimes to the surface. In the revised scheme precipitation from ice cloud is treated in a similar way as that from liquid cloud, i.e. it falls to the surface in a timestep, partly or completely evaporating on the way. (N.B. Neither of these ways of treating frozen precipitation is fully satisfactory from a theoretical point of view. A completely new large-scale ppn scheme is under development by S. Ballard and B. Golding but this will not be ready until next year.)

This change is considered essential since it alleviates the problems of excessive low cloud (level 1) being predicted in icy conditions although it doesnot entirely remove the

superadiabatic lapse rate.

Mod "B"

This is a change to improve the interaction of convection and boundary layer turbulent mixing. Currently the convection scheme adds *constant* specified excess temperature and humidity to the environment values to obtain the plume values used in initiation tests and initial mass flux calculations. The change replaces the constants, when initiating convection from the bottom model level (level 1) only, by the standard deviations of the turbulent fluctuations of temperature and humidity for level 1. The latter are calculated in terms of the surface sensible heat and moisture fluxes in the boundary layer mixing scheme.

Mod "C"

This modification also restricts the depth of non-local turbulent mixing but in a more radical way to mod "D". The top of the rapid mixing layer is constrained not to exceed the base of any convective cloud.

Mod "D"

This simple change just reduces the critical Richardson numbers used in diagnosing the top of the layer in which rapid non-local turbulent mixing occurs. It prevents the rapid mixing from encroaching too easily into stable layers. Thus it tends to restrict the depth of non-local mixing.

These modifications were tested by rerunning the limited area model forecast from DT06Z 5/1/94 which was known to suffer from the superadiabatic lapse rate problem. Mod 'A' was included in all reruns as it was considered an essential change. Nine model points in the superadiabatic area in the Atlantic were selected and tephigrams compared to see the impact of the modifications. All the modifications showed a marked improvement to the ascents but some combinations did not clear the superadiabatic lapse rates completely. Table 1 is a brief summary of the tests, showing how many tests points kept a superadiabatic lapse rate in the modified reruns.

forecast	Points with superadiabatic lapse rate problems	
	T+12 f/c from DT06Z 5/1/94	T+24 f/c from DT00Z 18/1/94
operational	9	3
mods 'AB'	0	1
mods 'AC'	5	0
mods 'AD'	7	1
mods 'ABC'	0	0
mods 'ABD'	0	0
mods 'ABCD'	0	0

TABLE 1. Summary of tests on two LAM forecasts using modifications to cure the

superadiabatic lapse rate problem.

Figures 3 a-e show the impact at 18Z 5/1/94 at 47N 14W for the five modification reruns 'AB','AC','AD','ABC' and 'ABD' respectively. From these results, mods 'AC' and 'AD' (Figures 3b and 3c) could be eliminated quickly as these reruns did not completely cure the super-adiabatic problem.

The tests were repeated for a second case, DT00Z 18/1/94, which proved to be a little more extreme. The ascents for the point 56N 17.5W for the four successful reruns from the previous case (mods 'AB','ABC','ABD','ABCD') are compared in Figure 4. The operational ascent, (Figure 4a), shows a slightly superadiabatic lapse rate between 700 and 800 hPa, with a comparatively warm, moist boundary layer. The impact of mod 'C' can be seen clearly from the ascents from the two reruns, mod 'ABC',(Figure 4c), and mod 'ABCD' (Figure 4e). Restricting the rapid mixing to below the convective cloud base resulted in a marked cooling of 2 degees at 800 hPa, making the ascents extremely cold and unstable. The impact of mod 'D' can be seen by comparing the lowest 100 hPa of the ascents in Figure 4b (mod 'AB') and Figure 4d (mod 'ABD') . Mod 'ABD' is preferred because the lowest layers are more unstable and the resulting precipitation is purely convective, rather than a mixture of dynamic and convective.

From the above tests, the best combinations of the modifications appear to be 'AB', 'ABC', 'ABD' or 'ABCD'.

LIMITED AREA TESTS ON SUMMER CONVECTION.
TRIAL PERIOD 12/9/94 - 30/9/94

The limited area model was rerun daily during this period using three combinations of the modifications in order to assess the impact on summer convection. The three versions run were mod 'AB', mod 'ABC' and mod 'ABD'. The reruns had a twelve-hour assimilation cycle but used the same observation and boundary files as the operational forecast.

Overall, the impact on mean sea level pressure / 500 hPa was small with no changes in forecast evolution. Depressions tended to be slightly deeper by 2-4 hPa at T+36/48. The main impact of the change was seen in differences in the distribution, intensity and frequency of showers. The mod 'AB' reruns were closest to the operational forecasts, whilst the mod 'ABC' and mod 'ABD' reruns showed a tendency for slightly more widespread showers and a slight deepening of depressions. The main differences noted are listed below in order of frequency.

(i) Showers slightly more widespread, especially in mod 'ABC' and mod 'ABD' reruns.
(ii) Depressions slightly deeper at T+36/48 by 2-4 hPa.
(iii) Increase in light precipitation / low cloud in cold unstable northerly airstream north of 60N.
(iv) Occasional showers heavier.
(v) Differences in light precipitation over the sea.

Two case studies are presented to illustrate differences in shower distribution.

a) T+36 forecast from DT00Z 12/9/94

The analysis in Figure 5a shows a depression in the southwest approaches moving towards Cornwall. The main band of rainfall associated with the depression didnot reach Cornwall until late afternoon. Ahead of this system, Southern England and Wales had a bright, mostly dry day, although, as the radar image for 12Z in Figure 5b shows, there were a few scattered showers over Wales and along the south coast. The operational T+36 forecast verifying at 12Z, shown in Figure 6a, gave a reasonable forecast for Southern England, although it predicted more showers than actually occurred. This tendency to over-predict showers was increased in all the trial forecasts, as can be seen by comparing the charts in Figure 6.

b) T+30/36 forecast from DT00Z 26/09/94

The analysis for 12Z 27th September, Figure 7a, shows a series of fronts moving southwards into Europe. the fronts have weakened over land, producing very little organised rain. However, scattered showers with isolated thunderstorms developed during the afternoon (thunderstorm reported at 49N 08E). The operational T+36 forecast verifying at 12Z, Figure 8 a, has predicted the potential instability correctly. The three trial forecasts have over-predicted the extent of the showers. Mod 'AB', Figure 8b, was similar to the operational forecast; Mod 'ABC', Figure 8b, predicted the heaviest showers (including a heavy shower symbol at 49N 08E); and mod 'ABD', Figure 8c, predicted the most showers.

In addition to the trial period 12th-30th September, the mods 'A','B','C' were also tested as part of the increased vertical resolution trial. Although this change could not be implemented operationally, it meant that the mods were assessed during the hottest time in the summer (June-August). The conclusions were very similar to those reached in this trial.

In the winter cases, mods 'AB', 'ABC','ABD' were most successful in clearing the super-adiabatic lapse rate. Since these mods are meant to enhance convection, it is to be expected that more showers would be predicted in the summer. The best combination for summer was 'AB'.

5. GLOBAL MODEL TESTS - trial week 07/01/94 - 13/01/94.

This week was chosen because the frozen physics package was introduced into the global model on 11th January. Shortly after this date, comments were received from forecasters in CFO about the model predicting dynamic rather than convective rainfall in showery airstreams. Investigations proved that this could also be attributed to the superadiabatic lapse rate problem. Figure 9b shows the total precipitation rate for the T+72 forecast verifying at 00Z 19th January 1994. Very cold unstable air is circulating around the depression over southeast Iceland. In spite of the 50% snow probability line being south of 50N between 20 W and 40W, the model is predicting mainly dynamic rain at most gridpoints north of 50N. The model ascent for one of these points is shown in

Figure 9a. This tephigram shows the same features seen in the limited area model; the very moist lowest levels, the warm 'nose' at the top of the boundary layer and the superadiabatic lapse rate between levels 6 and 7. The accumulations refer to the whole 72-hour period and they indicate that the model was predicting more dynamic rain than convective.

a) Modification tests

The same modification tests were carried out on two global forecasts, DT12Z 13/1/94 and DT00Z 16/1/94 as the superadiabatic lapse rate problem was known to be present in these cases. A number of model points in the superadiabatic area in the Atlantic were selected and tephigrams compared to see the impact of the modifications.

As in the LAM tests, all the modifications showed a marked improvement to the ascents but some combinations did not clear the superadiabatic lapse rates completely. Table 2 is a brief summary of the tests, showing how many tests points kept a superadiabatic lapse rate in the modified reruns.

forecast	Points with super-adiabatic lapse rate problems	
	T+132 f/c from DT12Z 13/1/94	T+72 f/c from DT00Z 16/1/94
operational	9	13
mods 'AB'	3	3
mods 'AC'	1	0
mods 'AD'	2	0
mods 'ABC'	0	0
mods 'ABD'	0	0
mods 'ABCD'	0	0

TABLE 1. Summary of tests on two global forecasts using modifications to cure the superadiabatic lapse rate problem.

From the global tests, mod 'AB' can be eliminated as not being a complete cure. Mods 'AC' and 'AD' were already eliminated from the limited area model trial. The most promising reruns were 'ABC', 'ABD','ABCD'.

b) Assessment of trial week 7th - 13th January 1994.

Modification 'ABD' was chosen for the trial week to improve the structure of the lowest 100mb of the boundary layer. Figure 10 shows the impact of this modification on the model T+72 forecast temperatures and precipitation. On the rainfall forecast chart, Figure 10b, most symbols in the cold unstable airmass ciculating around the depression are now convective. On the model ascent for the point 56N 17.5W, the super-diabatic lapse rate has been removed and the model is predicting convective rain.

Trial forecasts using the modification 'ABD' were rerun up to 6 days for the week 7th-13th January. In the assimilation, the original operational acobs files were used. The operational forecasts were also rerun using the current version of the model to act as a control. In Figure 11, we have used a quick diagnostic to show the immediate success of

the trial. It shows the number of grid points in the 6-day forecast run from DT00Z 7/1/94 in which theta decreased by more than 1K between levels 6 and 7. The graph shows a significant decrease in the number of such points in the trial forecast.

Impact on precipitation forecasts.

Rainfall statistics for the Northern Hemisphere at T+120, meaned over the period of the trial, showed an increase in convective precipitation and a smaller decrease in dynamic precipitation. The overall increase in total precipitation was 2.1%. The statistics also showed a small increase in frozen precipitation. Figures 12 a-c show the differences (trial - control) in the dynamic, convective and total accumulations for T+120 (meaned over the period 00Z 12/1/94 - 00Z 18/1/94) in the North Atlantic. Shaded areas indicate an increase in trial accumulations. The local increases in dynamic precipitation (Figure 12a) over East Greenland, the Newfoundland area and high ground in Europe ,e.g. the Alps, are partly due to changes in the ice fallout in mod 'C'. Increases in the convective precipitation over the sea, Figure 12b, are mainly due to the switch from dynamic to convective precipitation. As Figure 12c shows, the result of these changes is an overall increase in precipitation.

The main impact on precipitation seen by comparing individual forecasts were:

(i) A switch from dynamic rain to convective rain;
(ii) A increase in light snow north of 60N;
(iii) A small increase in the number of showers predicted;
(iv) A slight increase in the number of heavy showers predicted;
(v) Timing slightly faster at T+120/144.

In the tropics, an increase in convective rain and a small decrease in dynamic rain led to an overall increase in rainfall of 1.2%. Figures 13 a-c show the differences in the dynamic, convective and total accumulations for T+120 (meaned over the period 00Z 12/1/94 - 00Z 18/1/94) in the Tropics. Large differences (increases and decreases) in dynamic precipitation (Figure 13a) occurred mainly over high ground such as the Andes. Differences in convective rain were a result of increased showers overland over South America and South Africa. These differences were not very evident when comparing individual forecasts.

In the Southern Hemisphere, changes in precipitation were very small, and less than 0.1%.

Impact on mean sea level pressure forecasts.

Trial and control forecasts compared very closely up to T+ 72, but there were some changes in evolution T+96 onwards. No systematic differences were seen and this is confirmed by comparing the trial and control mean sea level pressure charts for the North Atlantic in Figures 14 (a) and (b) respectively. These charts have been obtained by calculating the mean pressure at T+120 over the trial week. Differences between the two charts are very small. However, there were some differences in the individual T+120 forecasts for the U.K. and two examples are described below.

The first example shows the largest difference seen at T+120 over the U.K. in the trial. The control and test T+120 mean sea level pressure forecasts for 00Z 13/1/94, Figures 15a and 15b respectively, show a significant difference over the U.K.. The control forecast has predicted a small depression, 978 hPa, over Northern Scotland with strong westerly winds over the U.K.. The test forecast has predicted a centre further south over Northern England, resulting in light winds. The analysis for 00Z 13/1/94, Figure 16a, shows that the control forecast was better in this case.

The second example illustated in Figures 17a and b, shows a typical difference at T+120 in the forecast depth of a depression in the southwest approaches. The test forecast, Figure 17b. is 4hPa deeper. Both are very good forecasts for T+120, although the verification analysis, Figure 16b, shows the actual position of the depression to be slightly closer to Southern Ireland.

6. OBJECTIVE VERIFICATION RESULTS

a) Limited Area Model - Period 13/09/94 - 29/09/94

A limited verification was performed for key parameters using the operational analyses. The key parameters were pressure at mean sea level, 500hPa height, 250hPa winds and temperatures and 850hPa temperatures. Forecasts for T+24 were verified for the whole limited area domain, and also for "area 5", the small region from Iceland to Northern Spain. Forecasts for T+48 were verified for the whole limited area domain only.

Figure 18 shows the T+24/48 bias and rms scores for mean sea level pressure. At T+24, the rms scores indicate a clear advantage to the operational forecasts, with 'AB' the best of the three trial forecasts. By T+48, however, the rms scores have levelled out, with only a minimal advantage to the operational forecasts. Changes in the biases are very small, with, if anything , a slight reduction in the biases of the trial forecasts.

The rms scores for 850 and 250 hPa temperatures, Figures 19 and 20 respectively, were very similar, with the operational forecasts verifying best at T+24, but this advantage becoming negligible by T+48.

In the 500 hPa verification, Figure21, the two trial forecasts, 'ABC' and 'ABD', have higher rms scores at T+24, which may be related to the small increase in showers over land. 'AB' is again the best of the trial forecasts. By T+48, all the scores have levelled out.

The verification for 250 hPa winds,(speed errors in Figure 22, vector errors in Figure 23) also show the same trend.

Of the three trial versions tried in the LAM summer trial, 'AB' verified the best. Unfortunately, global model trials indicated that 'AB' was not sufficient to clear all occurrences of the superadiabatic lapse rate.

b) Global Model Winter Trial Verification - Period 07/01/94 - 13/01/94

In the global model trial, model level temperatures, relative humidity and winds were verified against sonde observations. The results at T+72 and T+144 are presented in Figures 24-31. All the results shown verify at 00Z. The trial used mod 'ABD'.

i) Temperatures (T+72 Figure 24, T+144 Figure 25)

The trial and control temperatures were very close. The main impact in the Northern Hemisphere and Tropics was a slight increase in the cold bias at the surface and a very slight warming at level 5, 850 hPa. In the Southern Hemisphere, there was a slight warming at level5, 850 hPa,which reduced the model bias but also a slight cooling at levels 13 and 14, 200 hPa approx..

ii) Relative Humidities (T+72 Figure 26,T+144 Figure 27)

Again differences were very small. The main impact in the Northern Hemisphere was in the boundary layer, where the trial forecasts were very slightly drier.

iii) Westerly wind bias errors (T+72 Figure 28,T+144 Figure 29)

In the Northern Hemisphere at T+72, changes in the westerly wind bias errors were negligible. At T+144, errors against aireps were very slightly increased at levels 7-9, the levels most affected by the superadiabatic problem.

iv) Vector wind rms errors (T+72 Figure 30, T+144 Figure 31)

Differences in the rms scores against sondes were mainly negligible in the Northern Hemisphere. Against aireps, rms scores at T+144 were slightly improved for levels 9-14.

.

7. CONCLUSIONS

In outbreaks of very cold air in winter over a relatively warm sea (SST 8-10C), the model can predict occasional unrealistic ascents, with a super-adiabatic lapse rate above the boundary layer. The main cause of the super-adiabatic lapse rate is the interaction between the non-local mixing of heat and moisture in the boundary layer and the convection scheme. Too much mixing done by the rapidly mixing boundary layer removes most of the convective instability in the lower layers and suppresses convection. Very weak convection from the lower layers means insufficient convective heating at 700mb. The flux divergent ice fallout also exacerbates the problem.

The modifications described in section 3 are designed to correct this problem. The main points following from the limited area and global model tests are as follows:

1 Mod 'A' is considered necessary since it alleviates the problems of excessive low cloud (level 1) being predicted in icy conditions although it does not remove the super-adiabatic lapse rate.

2 A combination of at least three modifications was needed to clear all instances of

the superadiabatic lapse rate. The successful combinations were 'ABC','ABD' and 'ABCD'. Combination 'ABD' was chosen to be the best compromise.

3 Modification 'ABD' was chosen for the global trial to improve the structure of the lowest 100mb of the boundary layer.

4 Winter trials showed a clearance of the superadiabatic lapse rate, a switch to convective precipitation in cold unstable air over the sea, a slight increase in light snow showers, and an overall increase in convective precipitation. These are generally beneficial.

5 Summer tests with the limited area model indicated no changes in forecast evolution but a slight increase in the tendency to predict too widespread showers. Verification against operational analyses showed 'AB' to be the best of the three versions tried, but 'AB' did not clear all of the superadiabatic lapse rates in winter. For this 'ABD' was required, which verified slightly worse in summer.

6 In the global model winter trial, differences in mean sea level pressure forecasts were small up to T+72 but some evolution changes occurred at T+120/144. Verification was very similar to the operational (eg Fig 24, T+72 temperatures). There is a slight cooling at levels 1 and 2.

The combination of modifications 'ABD' is the best overall at reducing the occurrence of superadiabatic lapse rates and should be implemented operationally. The modifications 'AB' have already been implemented in the Autumn 1994 upgrade of the Mesoscale version of the forecast model. The prediction of showers by the LAM over the UK in the summer should be monitored and further changes sought to correct for the overprediction.

LIST OF FIGURES

Figure 1 (a) LAM T+12 f/c of mean sea level pressure and total precipitation rates verifying at 18Z 5/1/94
(b) LAM T+12 f/c tephigram at 47N 14Wverifying at 18Z 5/1/94

Figure 2 LAM T+12 tephigram at 47N 14Wverifying at 18Z 5/1/94
(a) - convection called every timestep
(b) - convective downdraught omitted
(c) - rapidly mixing boundary layer omitted
(d) - fully divergent ice scheme omitted

Figure 3 LAM T+12 tephigram at 47N 14Wverifying at 18Z 5/1/94
(a) - Mod 'AB' (b) - Mod 'AC' (c) - Mod 'AD'
(d) - Mod 'ABC' (e) - Mod 'ABD'

Figure 4 LAM T+24 tephigram at 56N 17.5Wverifying at 00Z 19/1/94
(a) - Operational (b) - Mod 'AB' (c) - Mod 'ABC'

(d) - Mod 'ABD' (e) - Mod 'ABCD'

Figure 5 (a) Analysis for 12Z 13/09/94 (b) Radar image for 12Z 13/09/94

Figure 6 LAM T+36 f/c of mean sea level pressure and total precipitation rates verifying at 12Z 13/09/94
(a) - operational (b) - Mod 'AB' (c) - Mod 'ABC'
(d) - Mod 'ABD'

Figure 7 (a) Analysis for 12Z 27/09/94
(b) Meteosat infra-red satellite imagery for 12Z 27/09/94

Figure 8 LAM T+36 f/c of mean sea level pressure and total precipitation rates verifying at 12Z 27/09/94
(a) - operational (b) - Mod 'AB' (c) - Mod 'ABC'
(d) - Mod 'ABD'

Figure 9 (a) Global model operational T+72 f/c tephigram for 56N 17.5Wverifying at 00Z 19/01/94
(b) Global model operational T+72 f/c of mean sea level pressure and total precipitation rates verifying at 00Z 19/01/94

Figure 10 (a) Global model trial (mod 'ABD') T+72 f/c tephigram for 56N 17.5W verifying at 00Z 19/01/94
(b) Global model trial (mod 'ABD') T+72 f/c of mean sea level pressure and total precipitation rates verifying at 00Z 19/01/94

Figure 11 Graph showing the number of superadiabatic points (DTHETA > 1.0K) at level 6 in the 6 day trial and control forecasts run from DT00Z 7/1/94

Figure 12 Differences in T+120 meaned accumulations in the North Atlantic:
(a) dynamic (b) convective (c) total

Figure 13 Differences in T+120 accumulations in the Tropics;
(a) dynamic (b) convective (c) total

Figure 14 Averaged mean sea level pressure forecast at T+120 for the trial week;
(a) trial (b) control (c) difference (a) - (b)

Figure 15 (a) T+120 operational f/c of mean sea level pressure and total precipitation rates verifying at 00Z 13/01/94
(b) T+120 trial (mod 'ABD') f/c of mean sea level pressure and total precipitation rates verifying at 00Z 13/01/94

Figure 16 (a) Mean sea level pressure analysis (operational) for 00Z 13/01/94
(b)Mean sea level pressure analysis (operational) for 00Z 15/01/94

Figure 17 (a) T+120 operational f/c of mean sea level pressure and total precipitation rates verifying at 00Z 15/01/94
(b) T+120 trial (mod 'ABD') f/c of mean sea level pressure and total precipitation rates verifying at 00Z 15/01/94

LAM objective verification results - Period 13/09/94 - 29/09/94

Figure 18 Verification of mean sea level forecasts at T+24/48 against operational analyses.

Figure 19 Verification of 850 hPa temperatures at T+24/48 against operational

Figure 20 Verification of 250 hPa temperatures at T+24/48 against operational analyses.

Figure 21 Verification of 500 hPa heights at T+24/48 against operational analyses.

Figure 22 Verification of 250 hPa wind speed at T+24/48 against operational analyses.

Figure 23 Verification of 250 hPa vector winds at T+24/48 against operational analyses.

Global Model objective verification results -- Period 07/01/94 -- 13/01/94

Figure 24 Model level temperatures verified against sonde temperatures at T+72.

Figure 25 Model level temperatures verified against sonde temperatures at T+144.

Figure 26 Model level relative humidities verified against sonde humidities at T+72.

Figure 27 Model level relative humidities verified against sonde relative humidities at T+144.

Figure 28 Model W wind bias errors against sonde winds at T+72.

Figure 29 Model W wind bias errors against sonde winds at T+144.

Figure 30 Model vector wind rms errors against sonde winds at T+72.

Figure 31 Model vector wind rms errors against sonde winds at T+144.

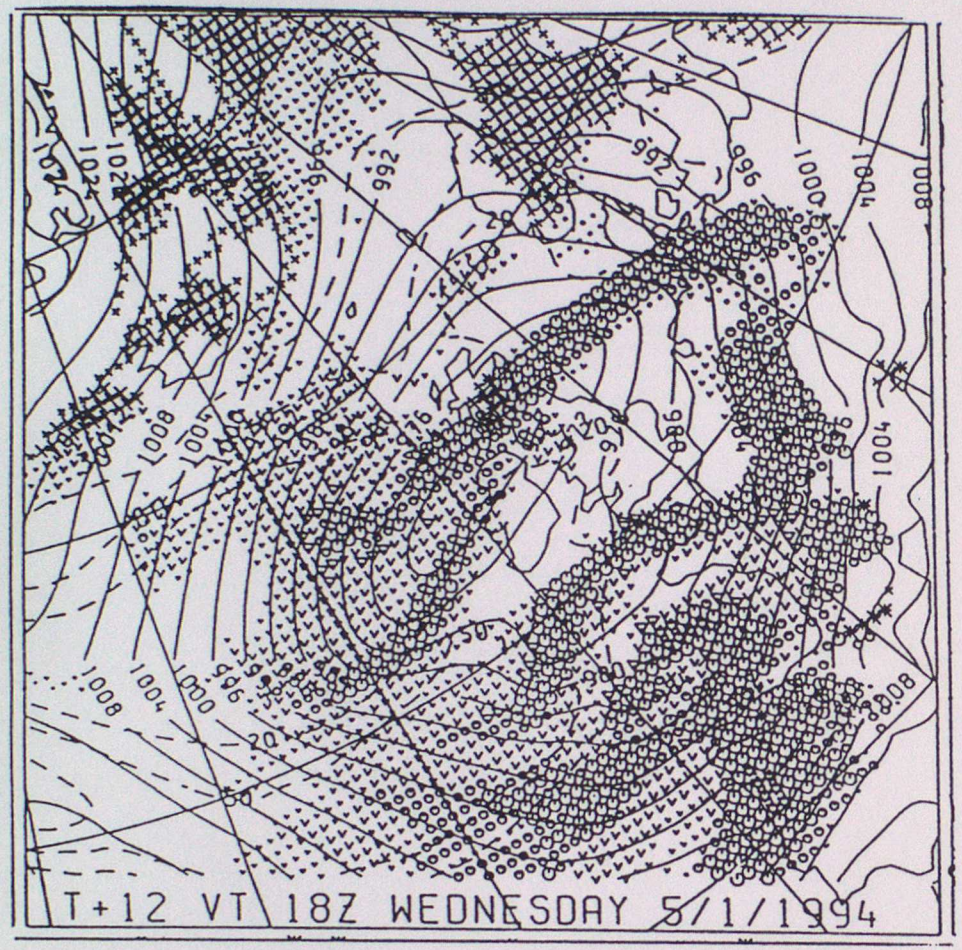

(a)

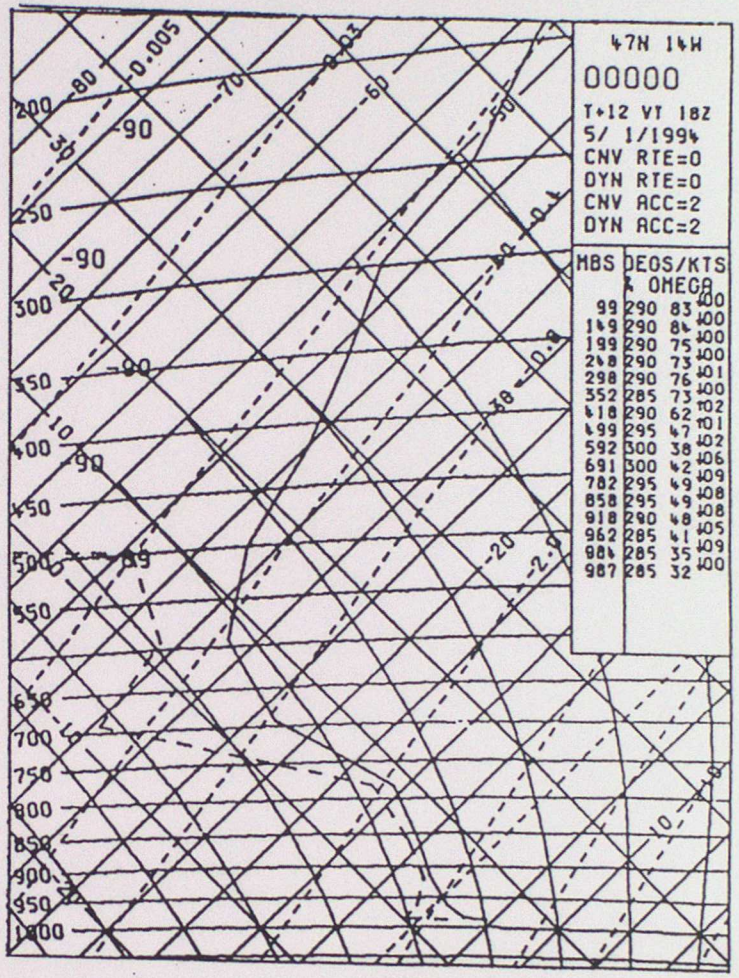

(b)

Figure 1 (a) LAM T+12 f/c of mean sea level pressure and total precipitation rates verifying at 18Z 5/1/94
(b) LAM T+12 f/c tephigram at 47N 14W verifying at 18Z 5/1/94

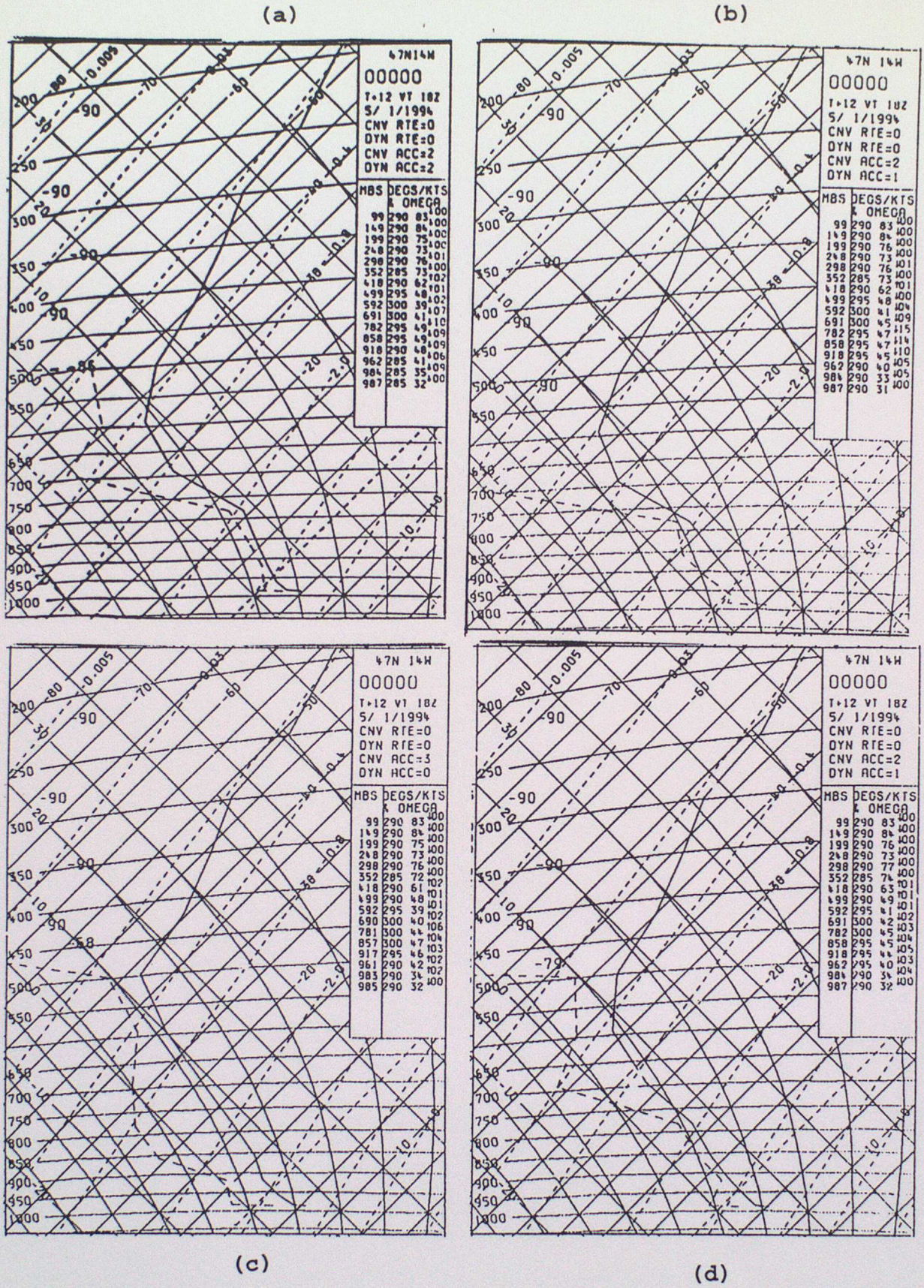

Figure 2 LAM T+12 tephigram at 47N 14W verifying at 18Z 5/1/94
(a) - convection called every timestep
(b) - convective downdraught omitted
(c) - rapidly mixing boundary layer omitted
(d) - fully divergent ice scheme omitted

(a)

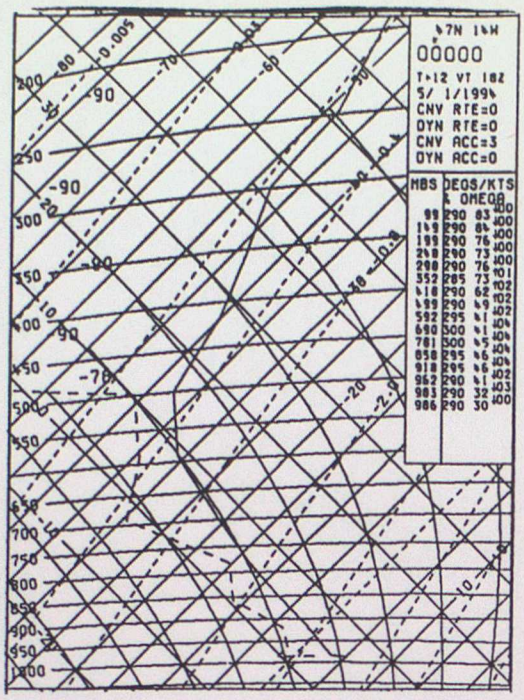

(b)

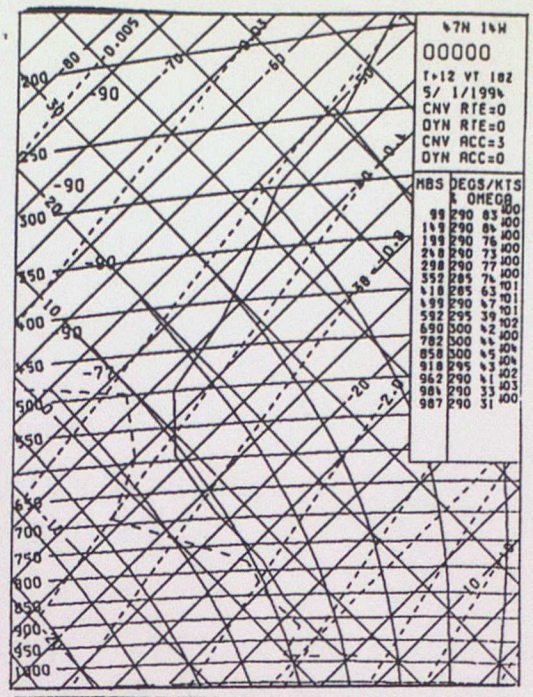

(c)

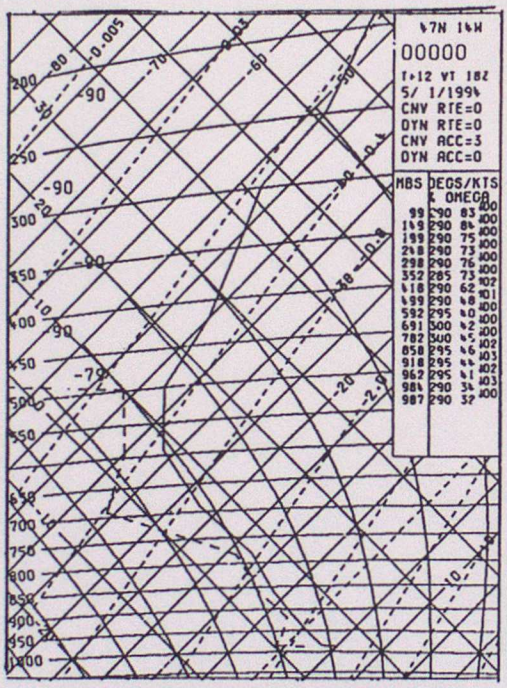

(d)

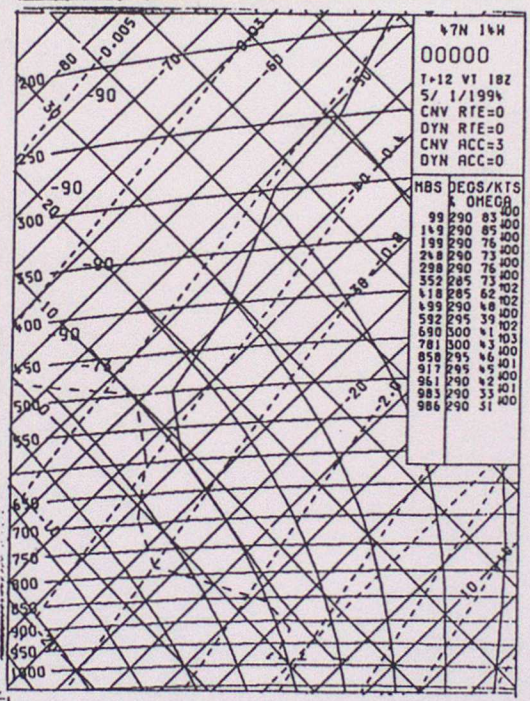

(e)

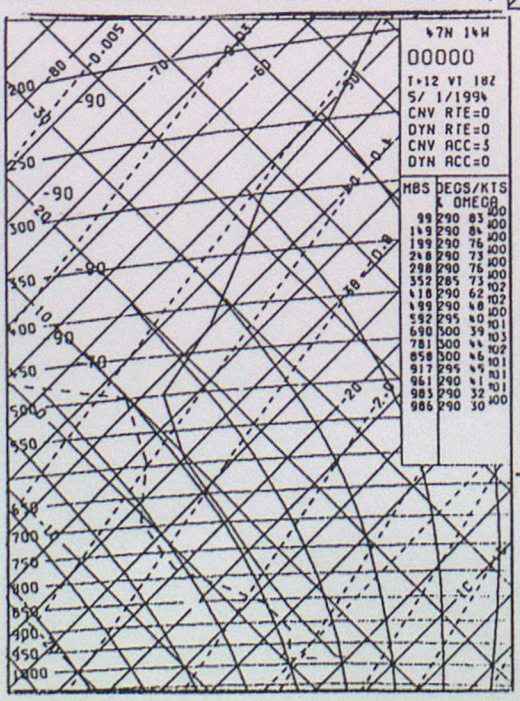

FIGURE 3
LAM T+12 tephigram at 47N 14W verifying at 18Z 5/1/94
(a) - Mod 'AB'
(b) - Mod 'AC'
(c) - Mod 'AD'
(d) - Mod 'ABC'
(e) - Mod 'ABD'

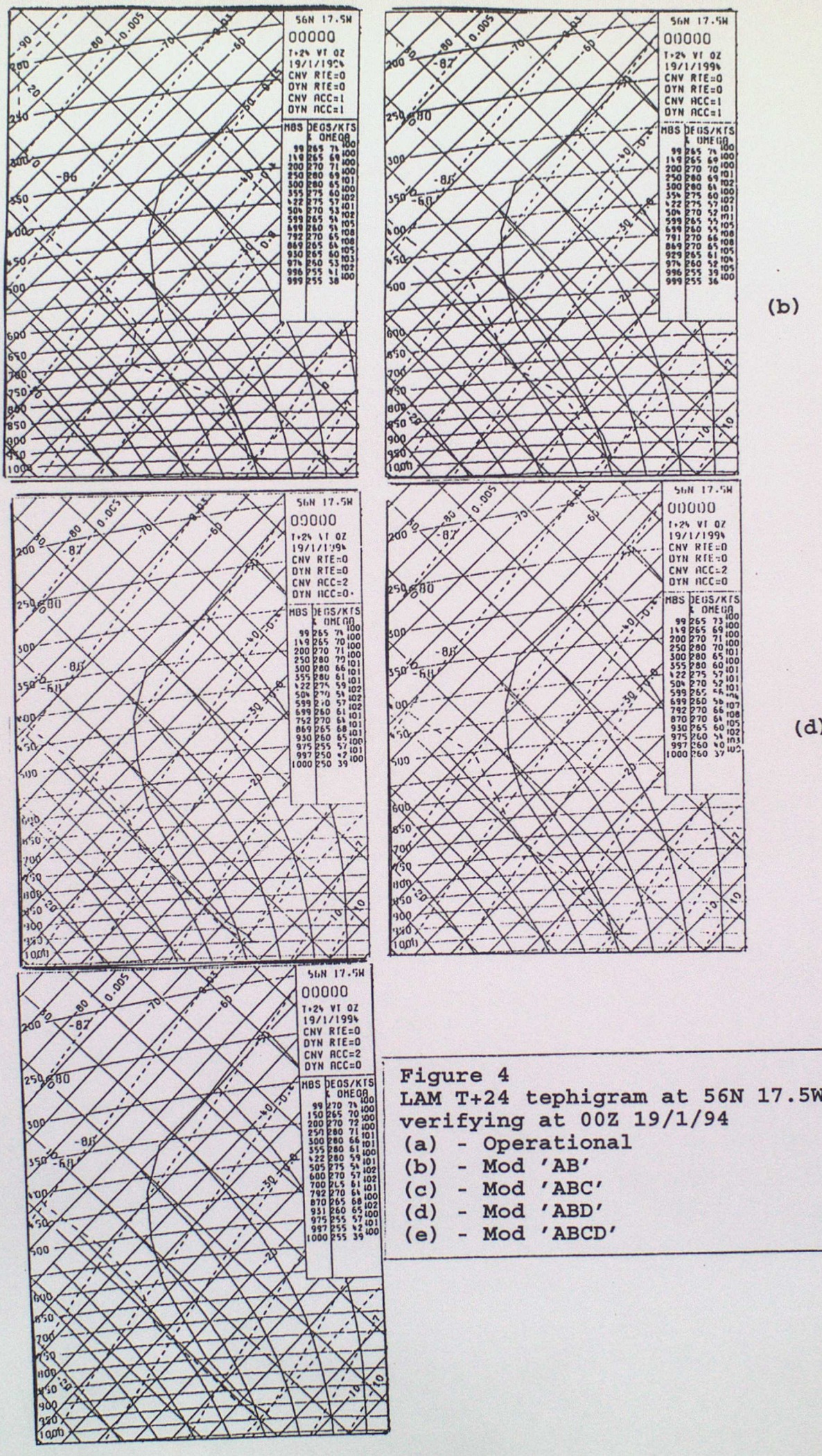

Figure 4
LAM T+24 tephigram at 56N 17.5W verifying at 00Z 19/1/94
(a) - Operational
(b) - Mod 'AB'
(c) - Mod 'ABC'
(d) - Mod 'ABD'
(e) - Mod 'ABCD'

(a)

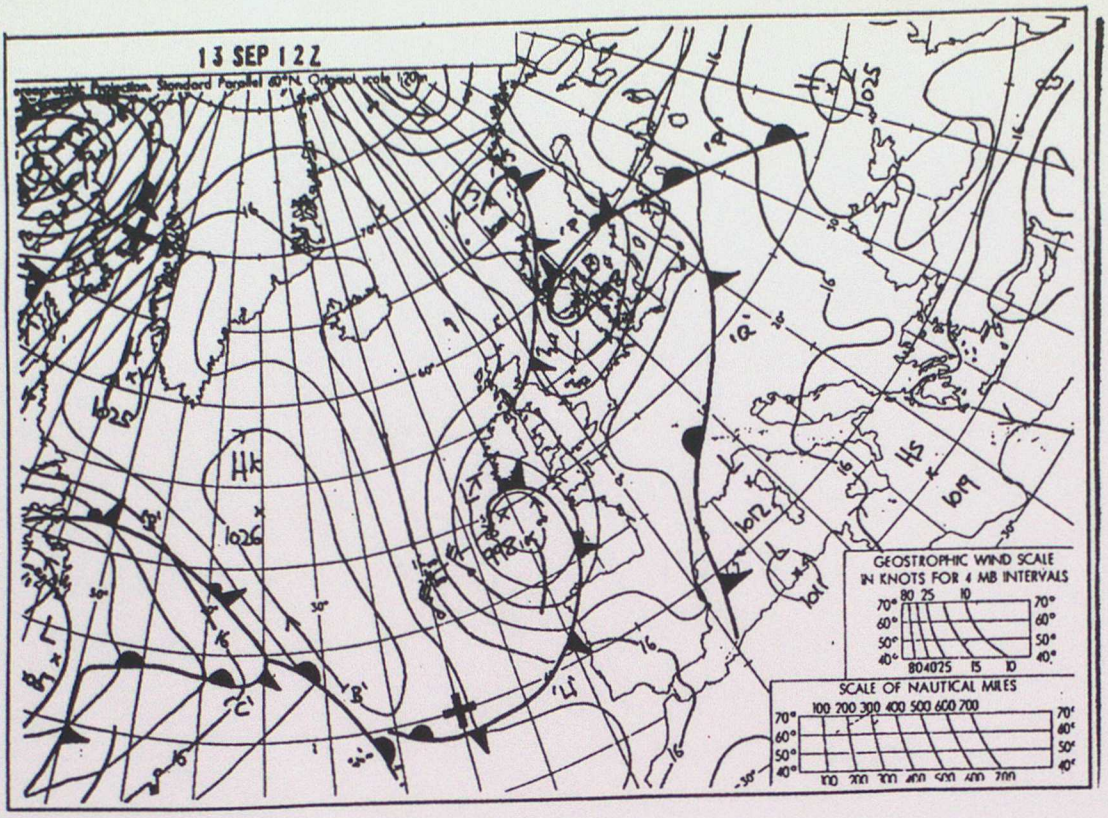

(b)

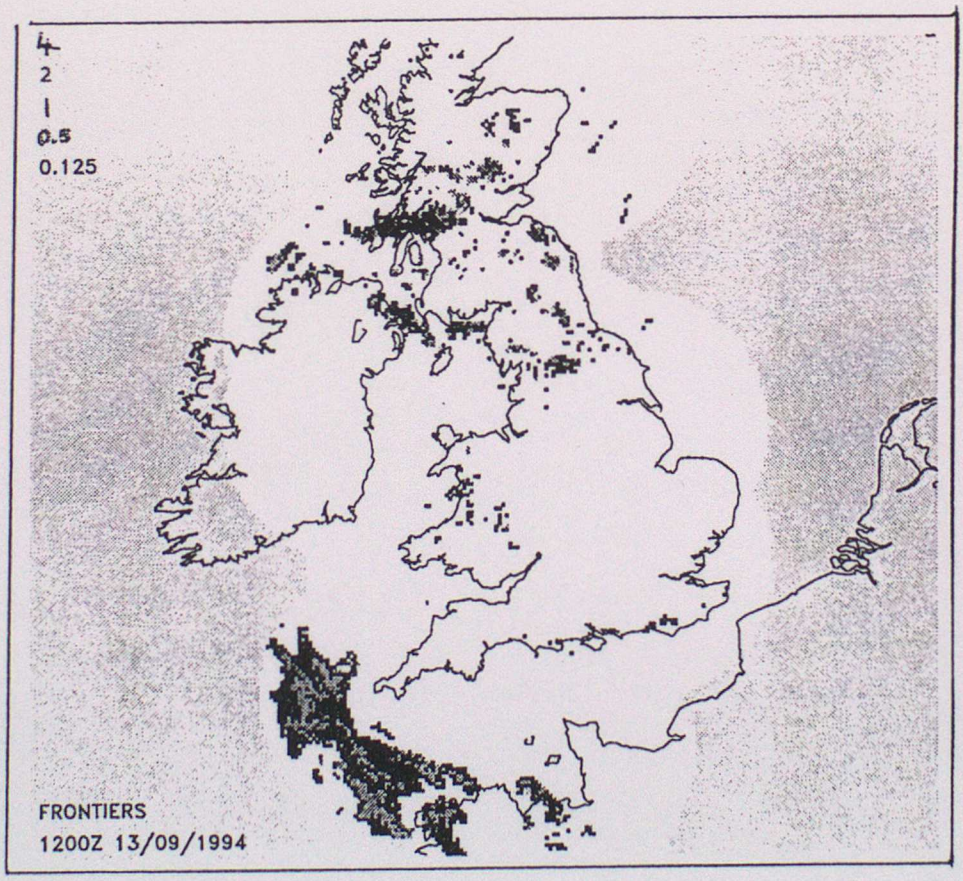

Figure 5 (a) Analysis for 12Z 13/09/94
(b) Radar image for 12Z 13/09/94

(a)

(b)

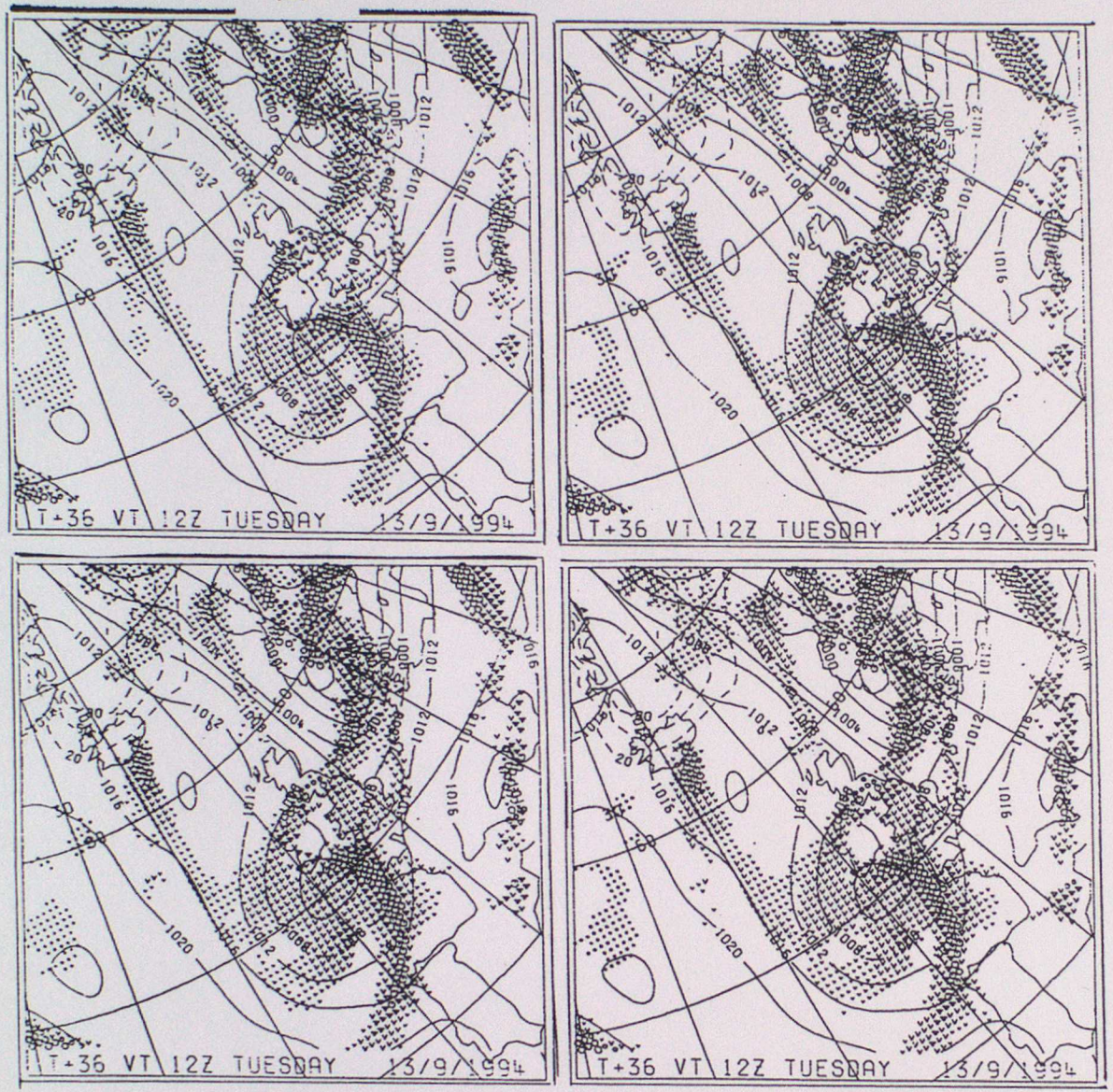

(c)

(d)

Figure 6
LAM T+36 f/c of mean sea level pressure and total precipitation rates verifying at 12Z 13/09/94
(a) - operational
(b) - Mod 'AB'
(c) - Mod 'ABC'
(d) - Mod 'ABD'

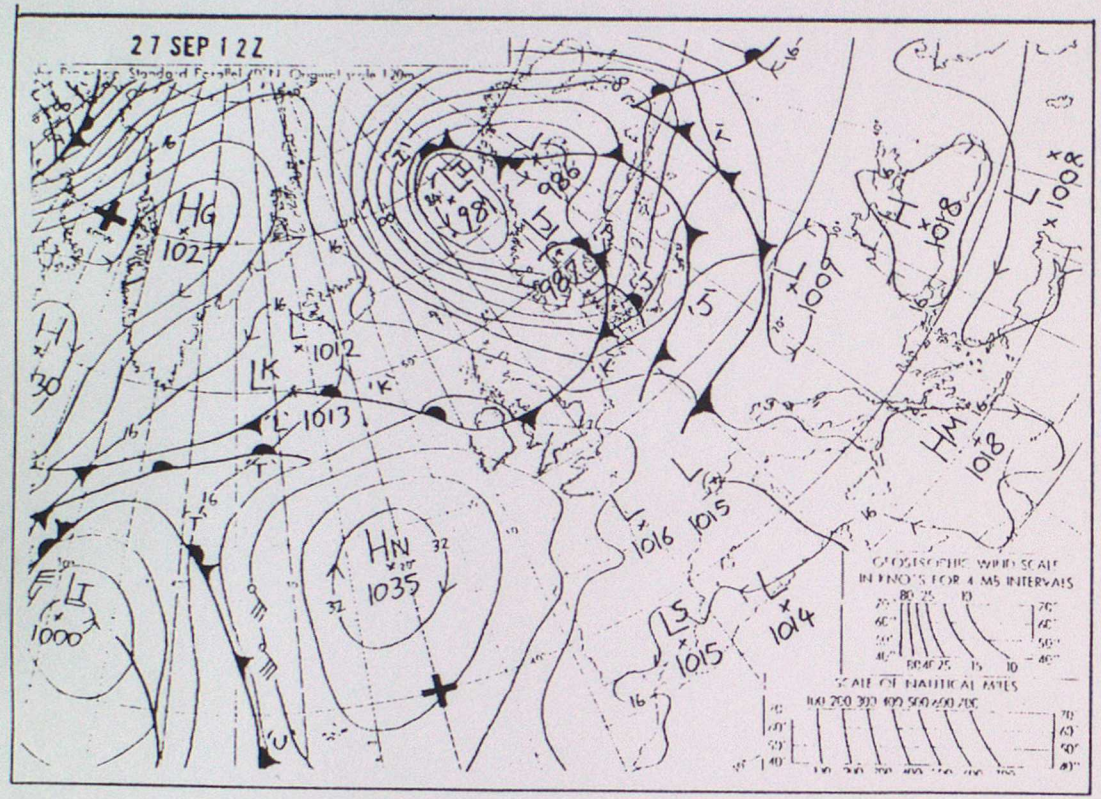

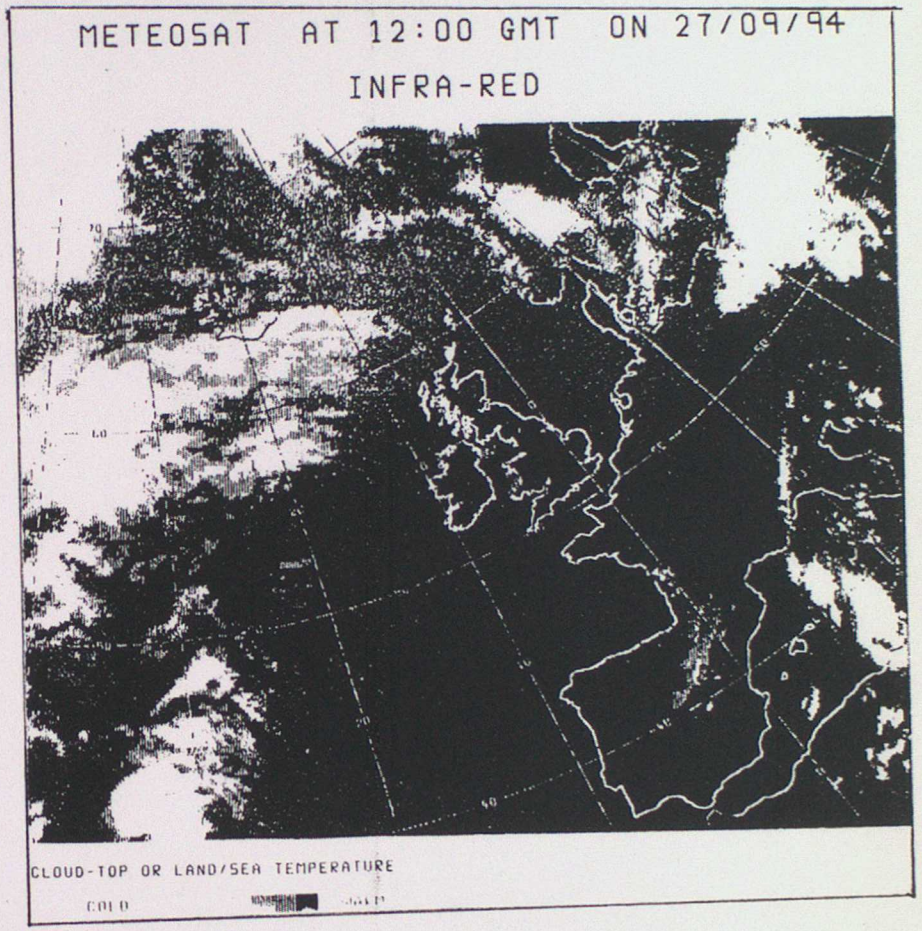

Figure 7 (a) Analysis for 12Z 27/09/94
(b) Meteosat infra-red satellite imagery for 12Z 27/09/94

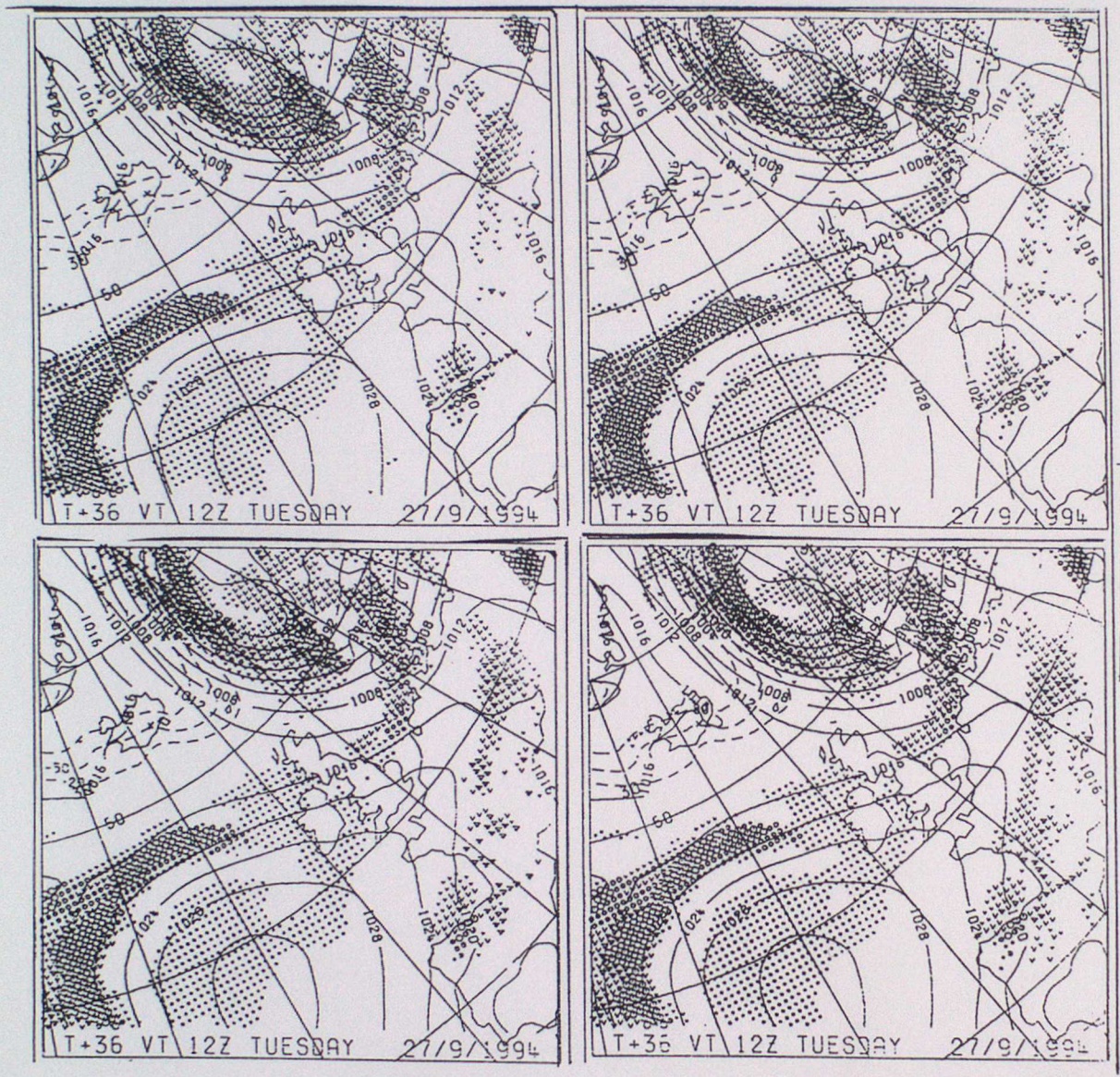

Figure 8
LAM T+36 f/c of mean sea level pressure and total precipitation rates verifying at 12Z 27/09/94
(a) - operational
(b) - Mod 'AB'
(c) - Mod 'ABC'
(d) - Mod 'ABD'

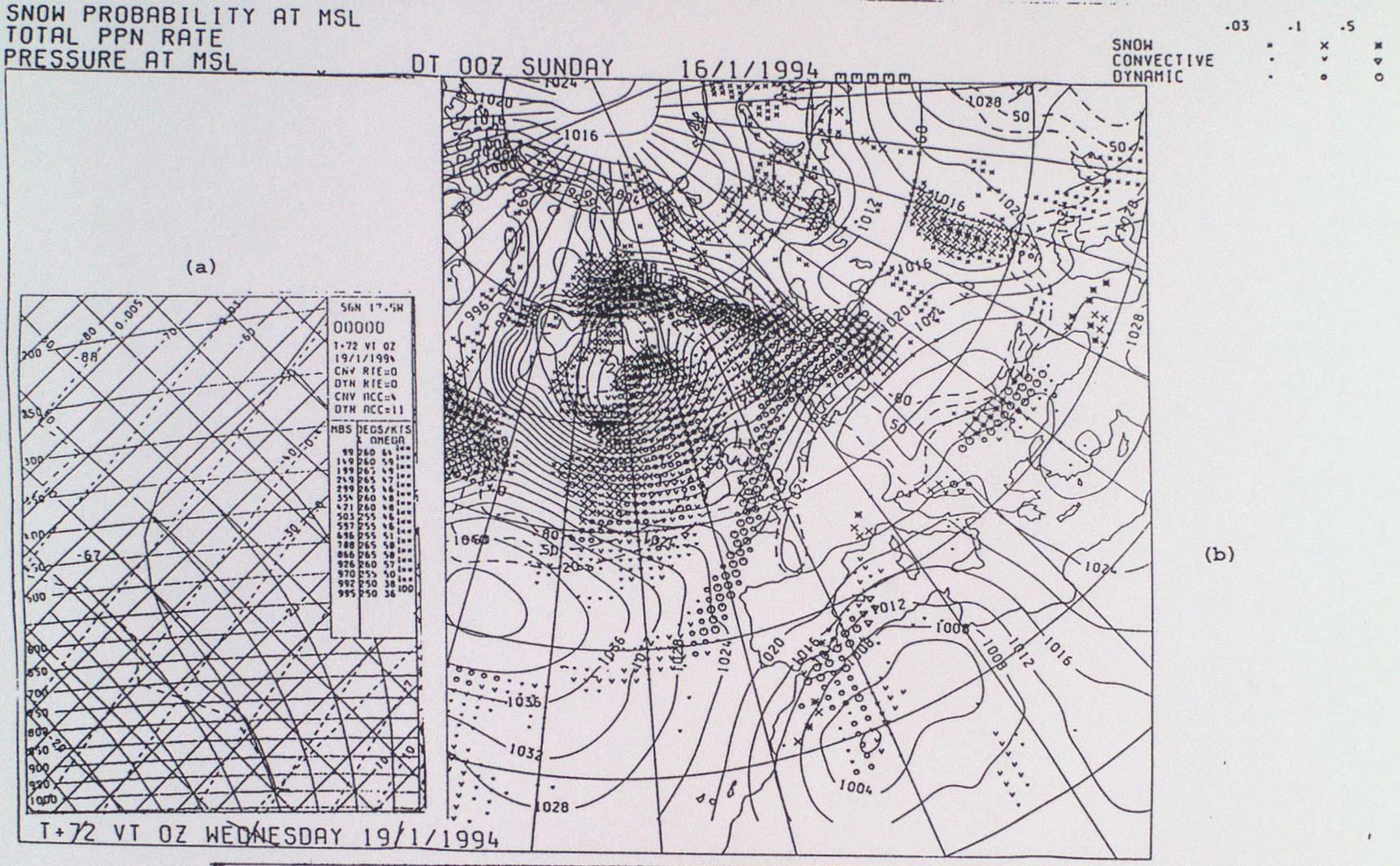

Figure 9 (a) Global model operational T+72 f/c tephigram for 56N 17.5Wverifying at 00Z 19/01/94
(b) Global model operational T+72 f/c of mean sea level pressure and total precipitation rates verifying at 00Z 19/01/94

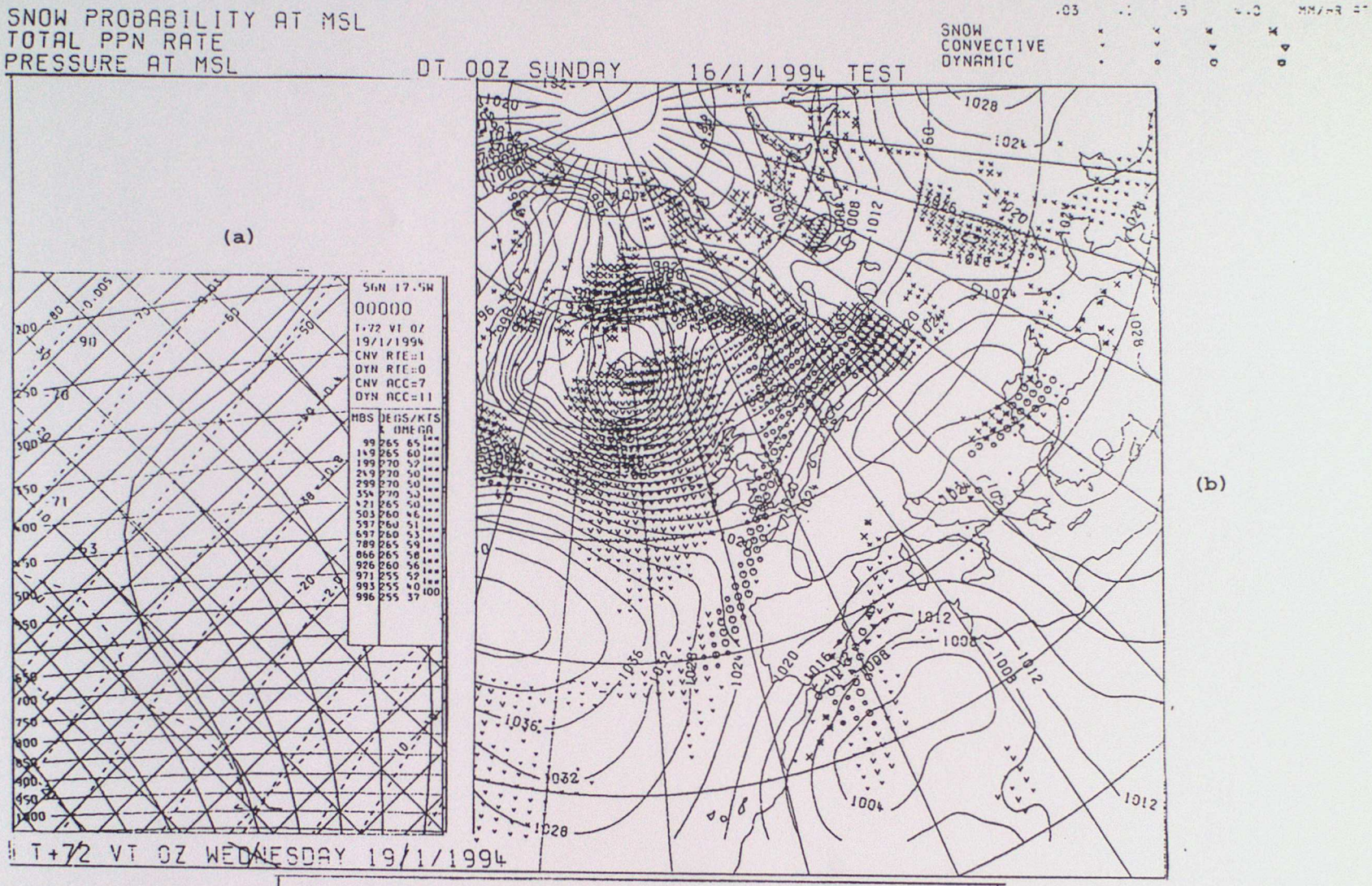

Figure 10
(a) Global model trial (mod 'ABD') T+72 f/c tephigram for 56N 17.5W verifying at 00Z 19/01/94
(b) Global model trial (mod 'ABD') T+72 f/c of mean sea level pressure and total precipitation rates verifying at 00Z 19/01/94

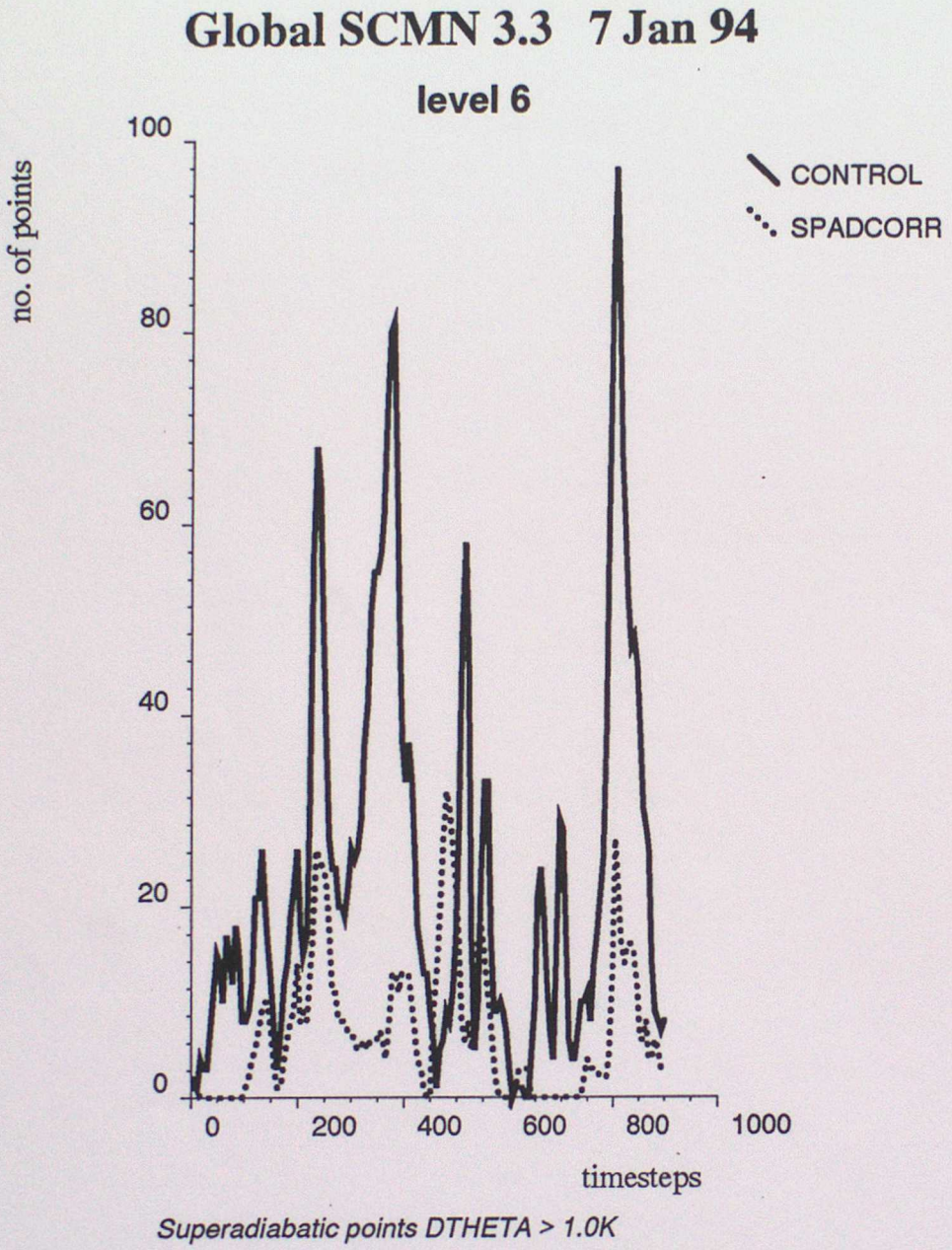

Figure 11 Graph showing the number of superadiabatic points (DTHETA>1.0K) at level 6 in the 6 day trial and control forecasts run from DT00Z 7/1/94

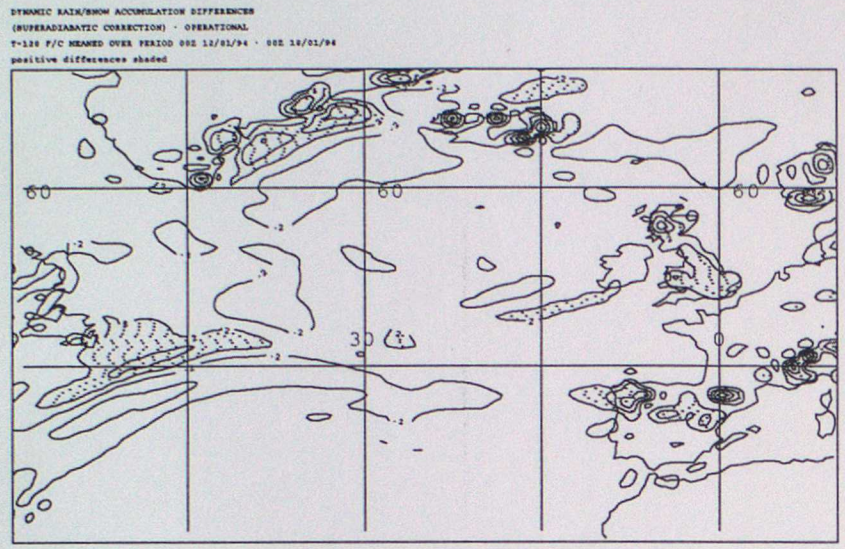

(a)

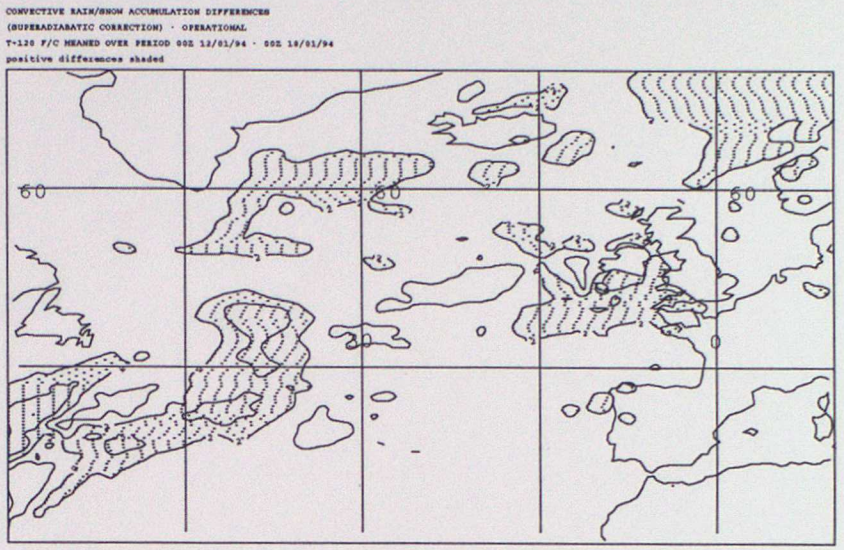

(b)

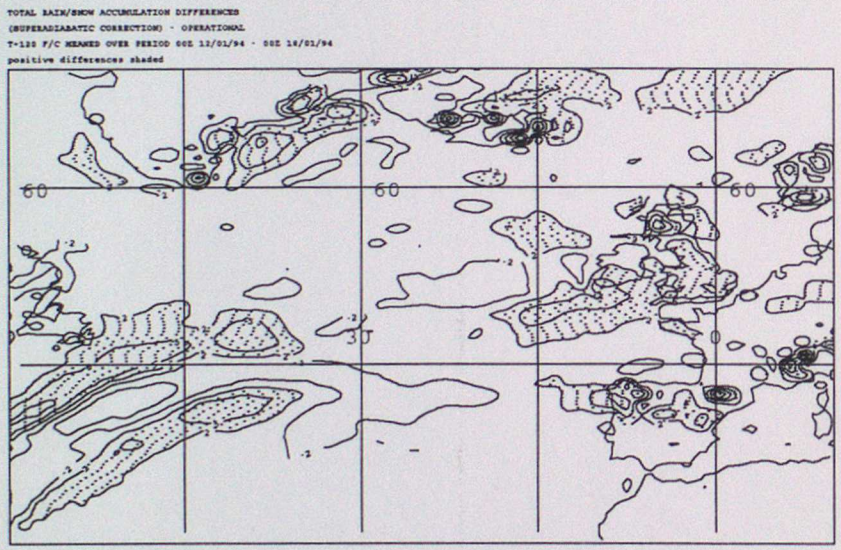

(c)

Figure 12
Differences in T+120 meaned accumulations in the North Atlantic:
(a) dynamic
(b) convective
(c) total

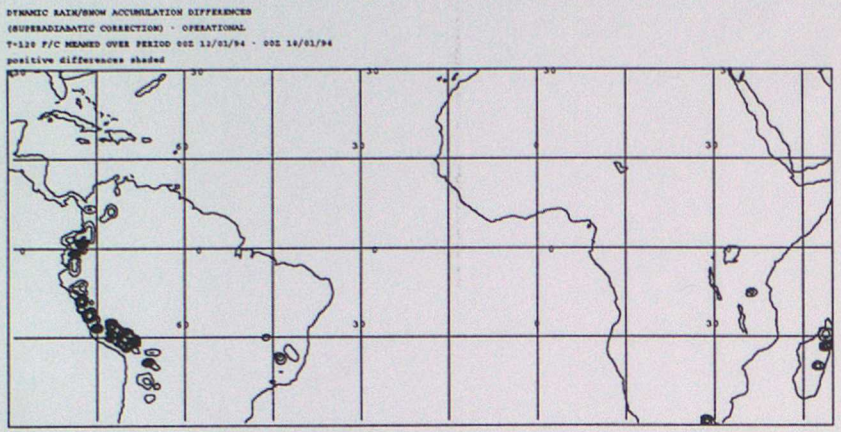

(a)

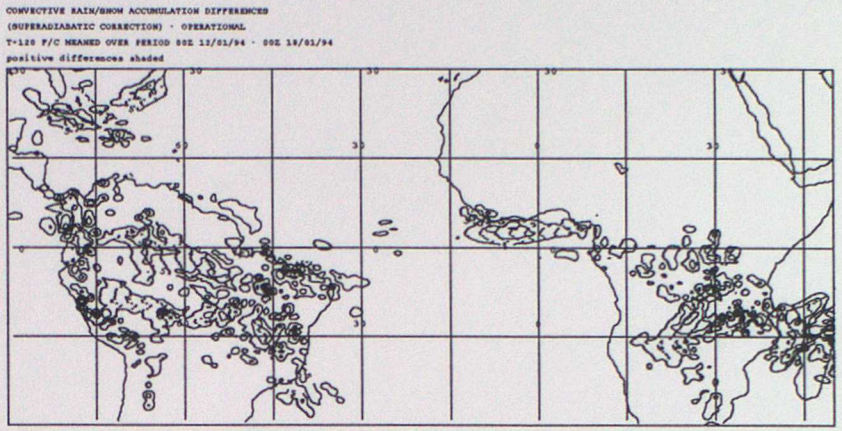

(b)

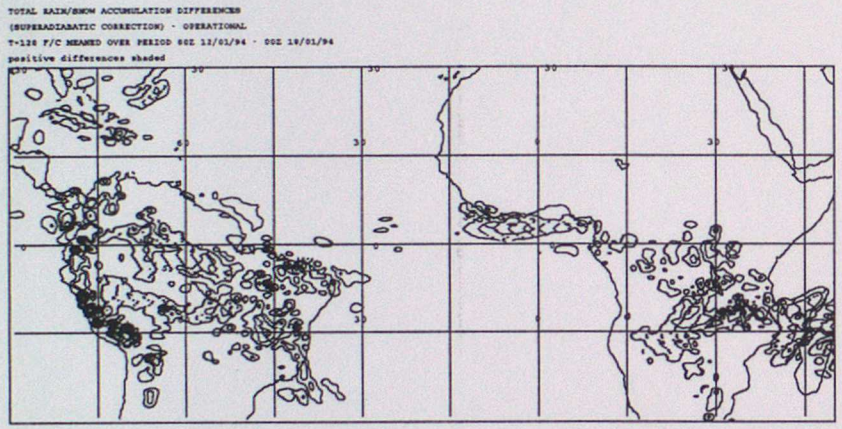

(c)

Figure 13
Differences in T+120 accumulations in the Tropics;
(a) dynamic
(b) convective
(c) total

(a)

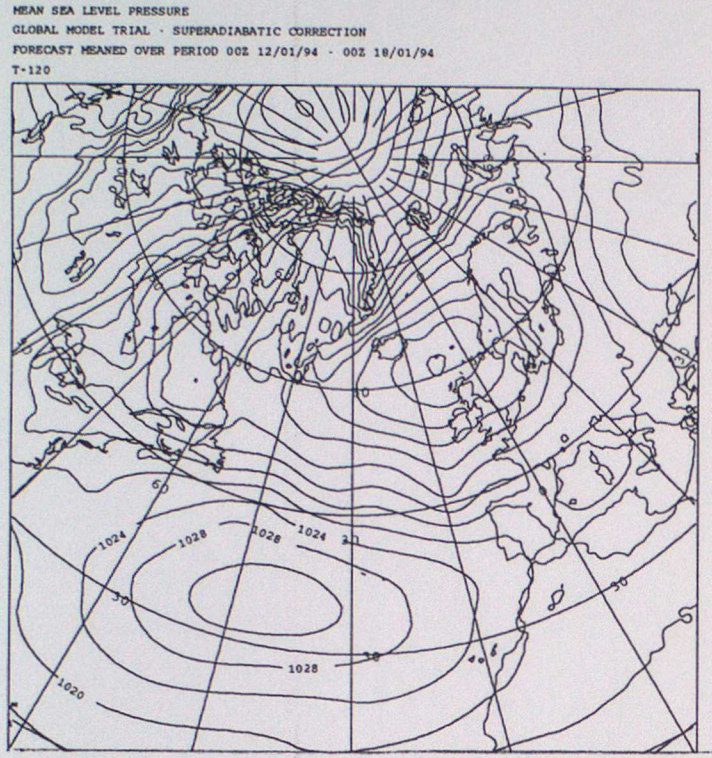

(b)

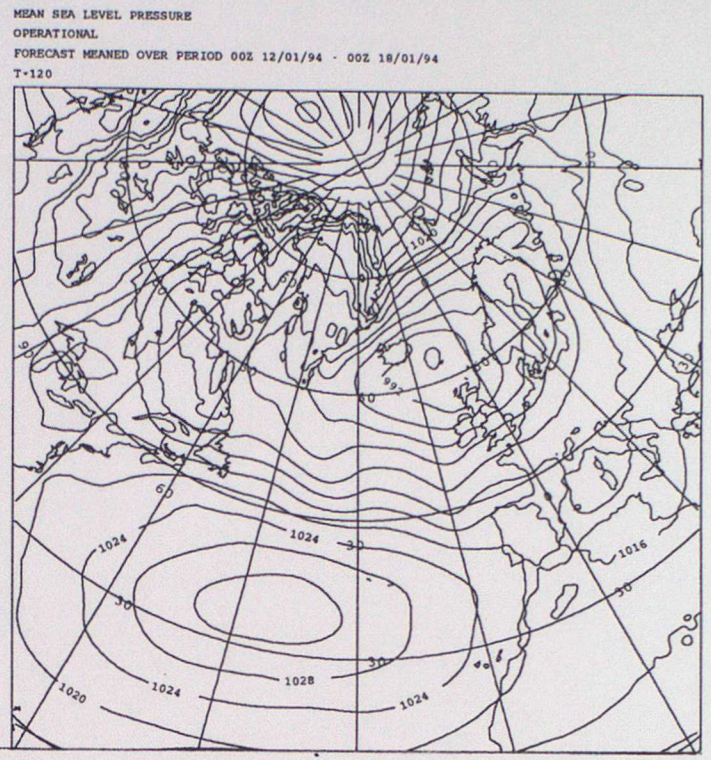

(c)

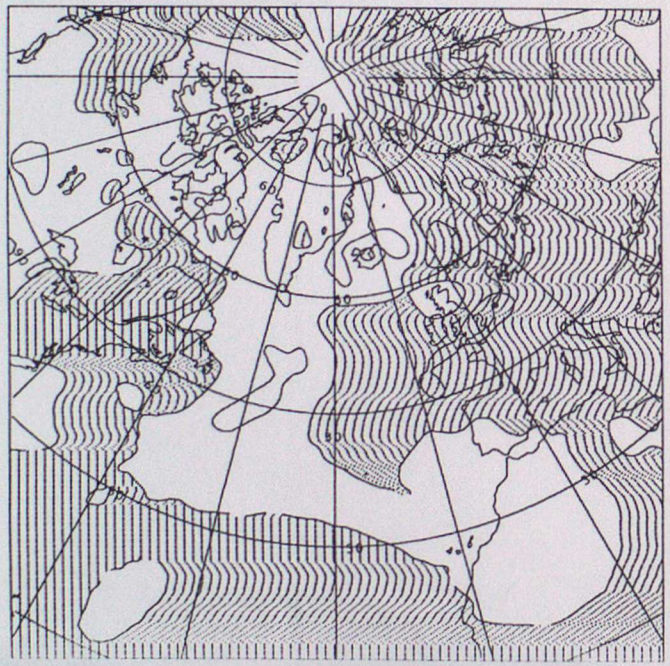

Figure 14
Averaged mean sea level pressure forecast at T+120 for the trial week (VT 00X 12/1/94 - 00Z 18/1/94
(a) trial
(b) control
(c) difference

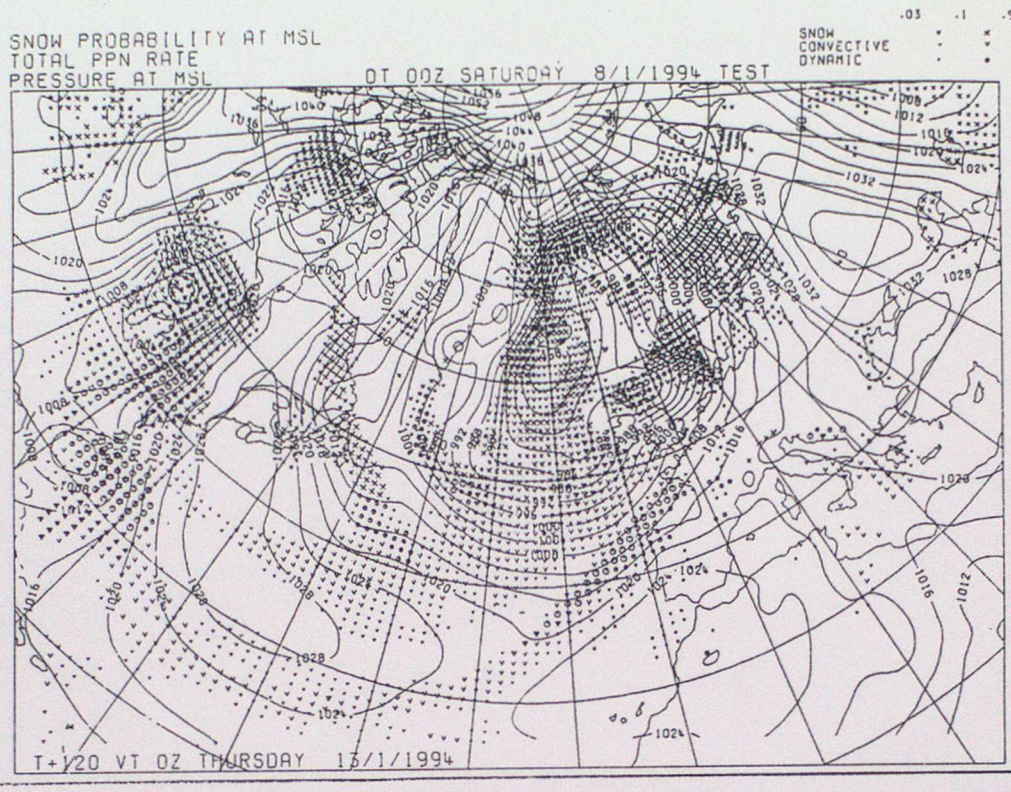

Figure 15 (a) T+120 operational f/c of mean sea level pressure and total precipitation rates verifying at 00Z 13/01/94

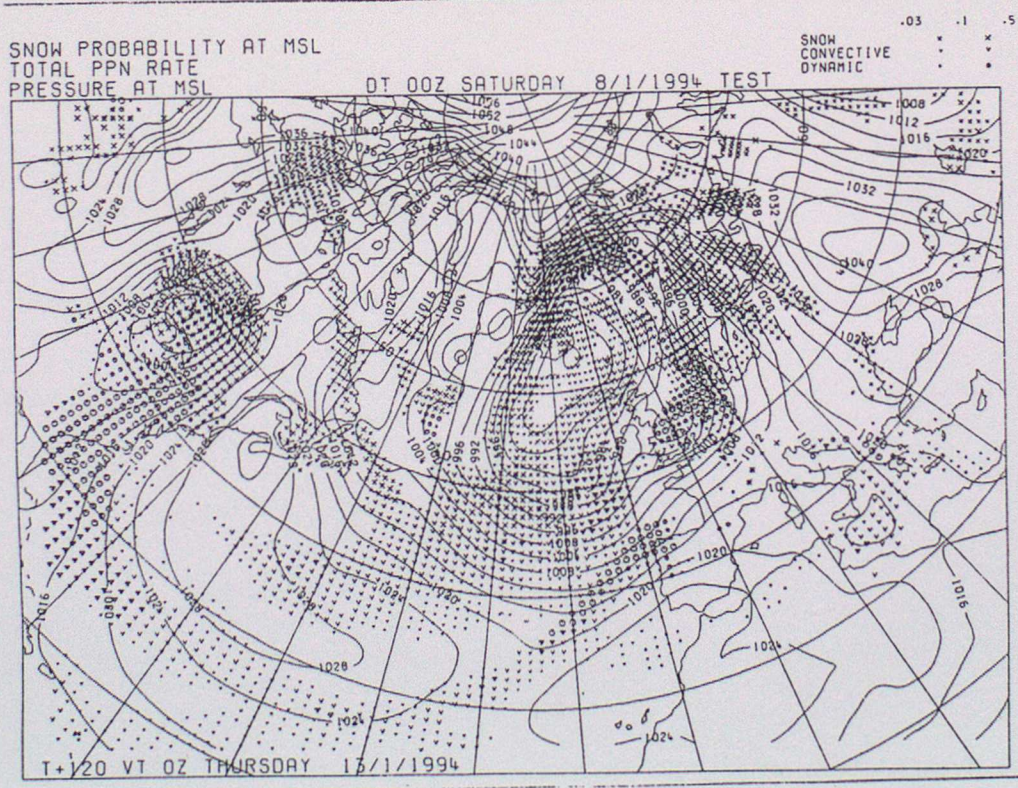

Figure 15 (b) T+120 trial (mod 'ABD') f/c of mean sea level pressure and total precipitation rates verifying at 00Z 13/01/94

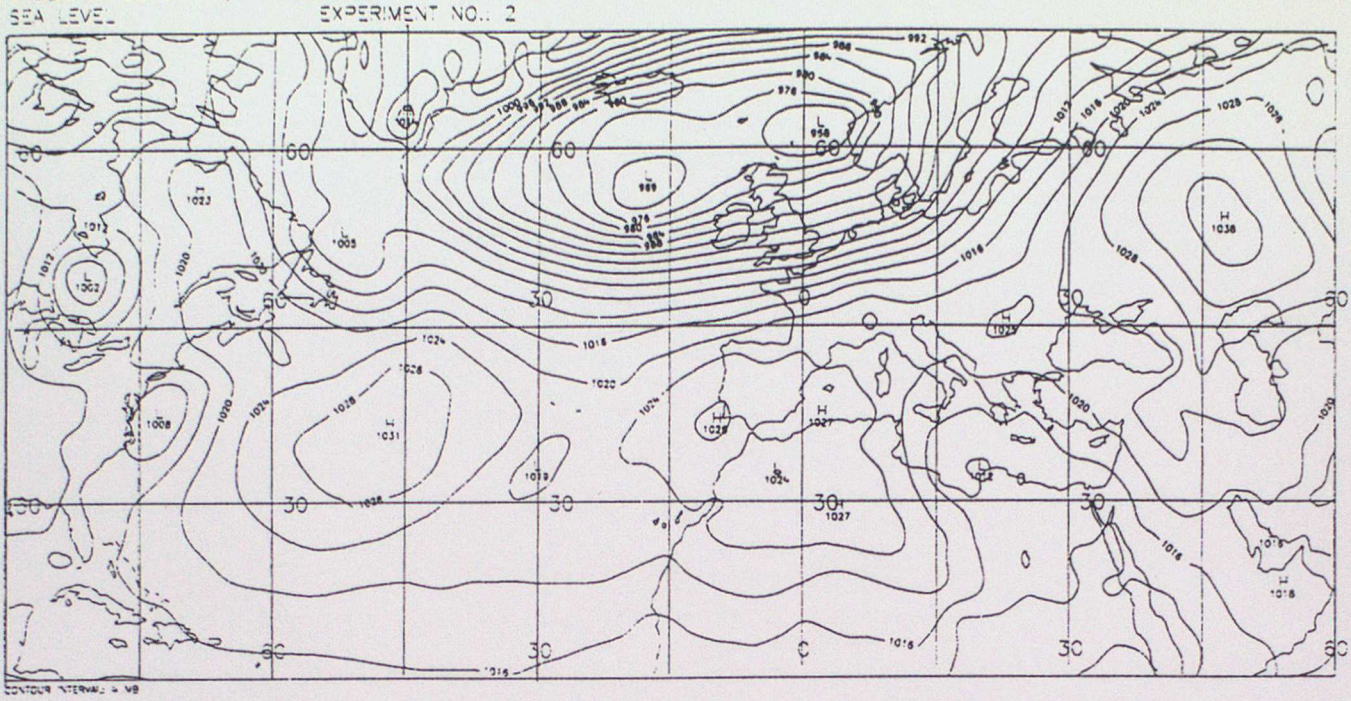

(a)

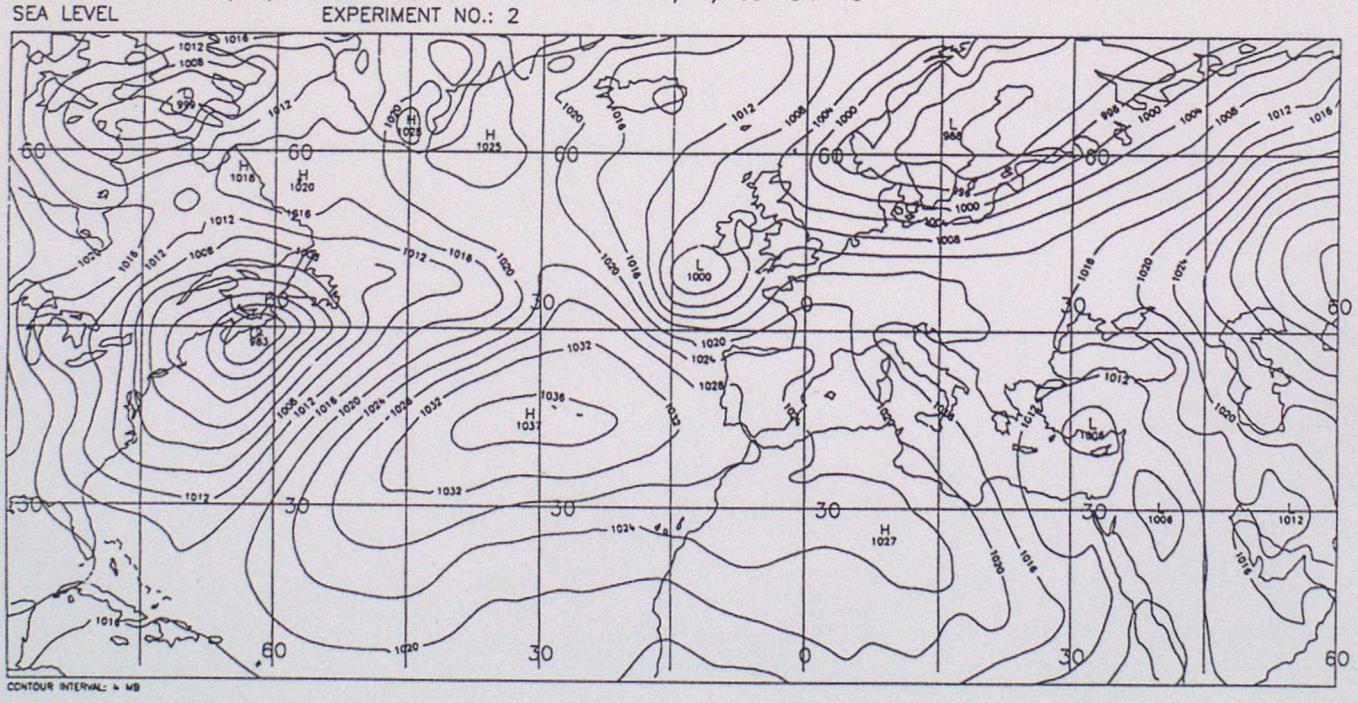

(b)

Figure 16 (a) Mean sea level pressure analysis (operational) for 00Z 13/01/94
(b) Mean sea level pressure analysis (operational) for 00Z 15/01/94

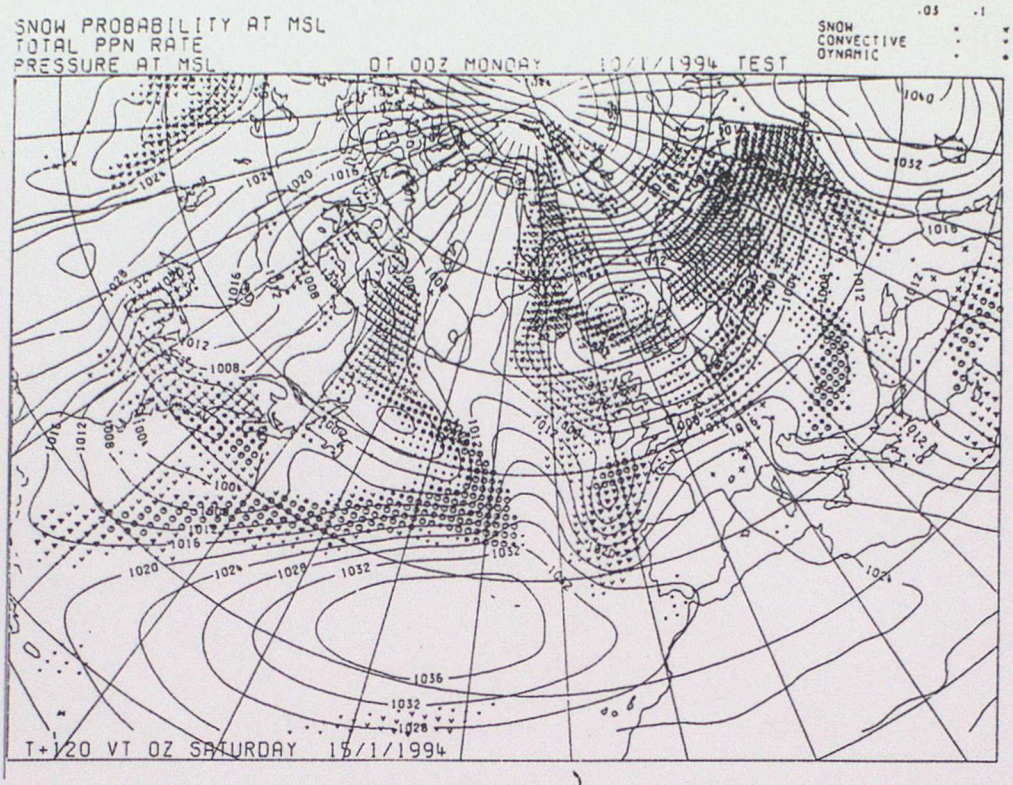

(a)

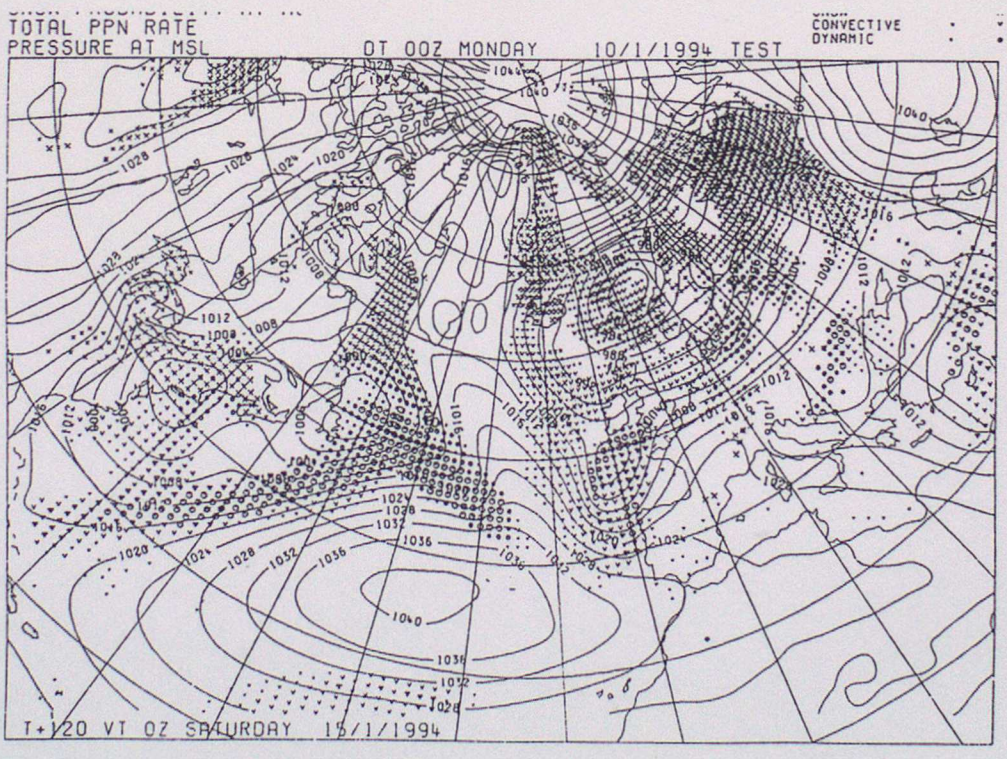

(b)

Figure 17 (a) T+120 operational f/c of mean sea level pressure and total precipitation rates verifying at 00Z 15/01/94
(b) T+120 trial (mod 'ABD') f/c of mean sea level pressure and total precipitation rates verifying at 00Z 15/01/94

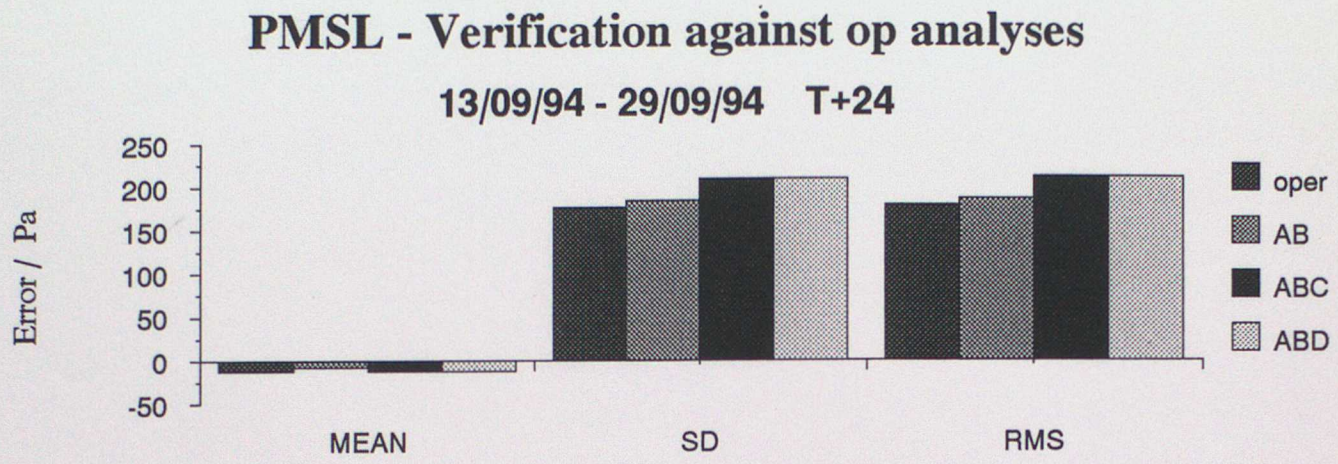

LAM domain

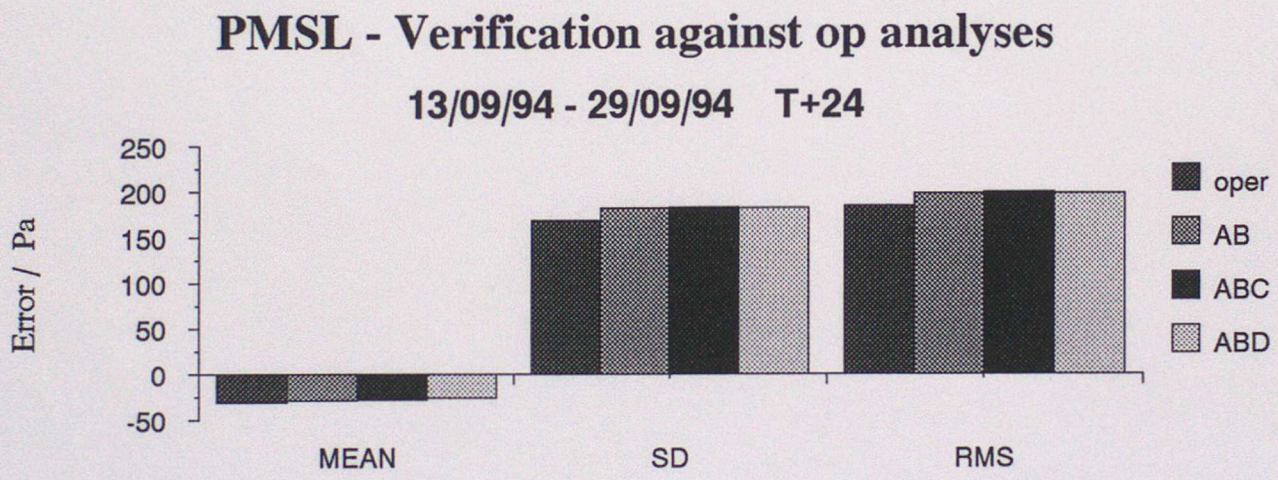

Area 5 domain

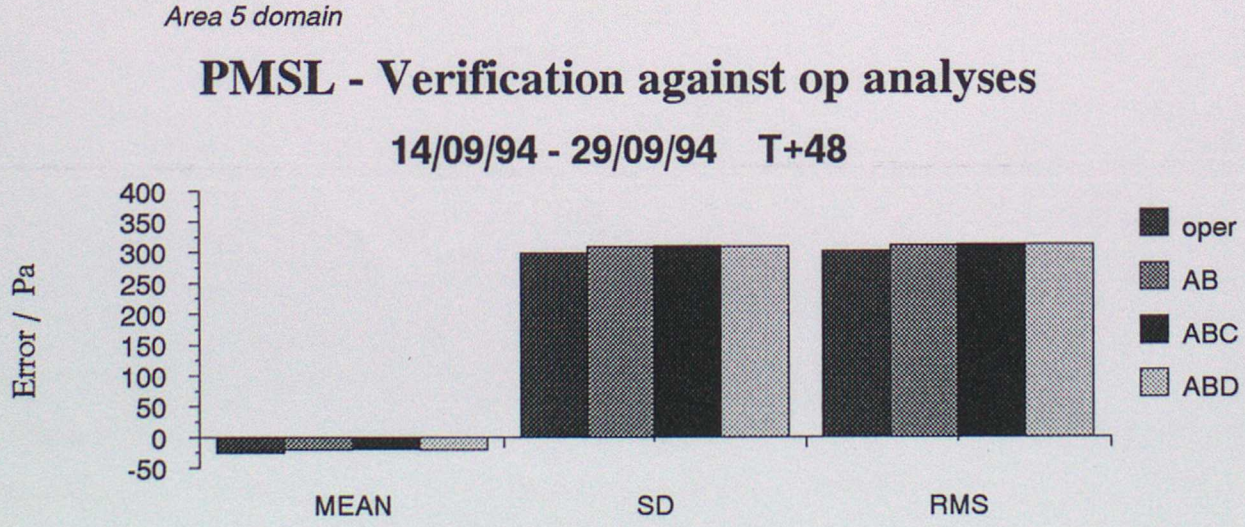

LAM domain

Figure 18 Verification of mean sea level forecasts at T+24/48 against operational analyses.

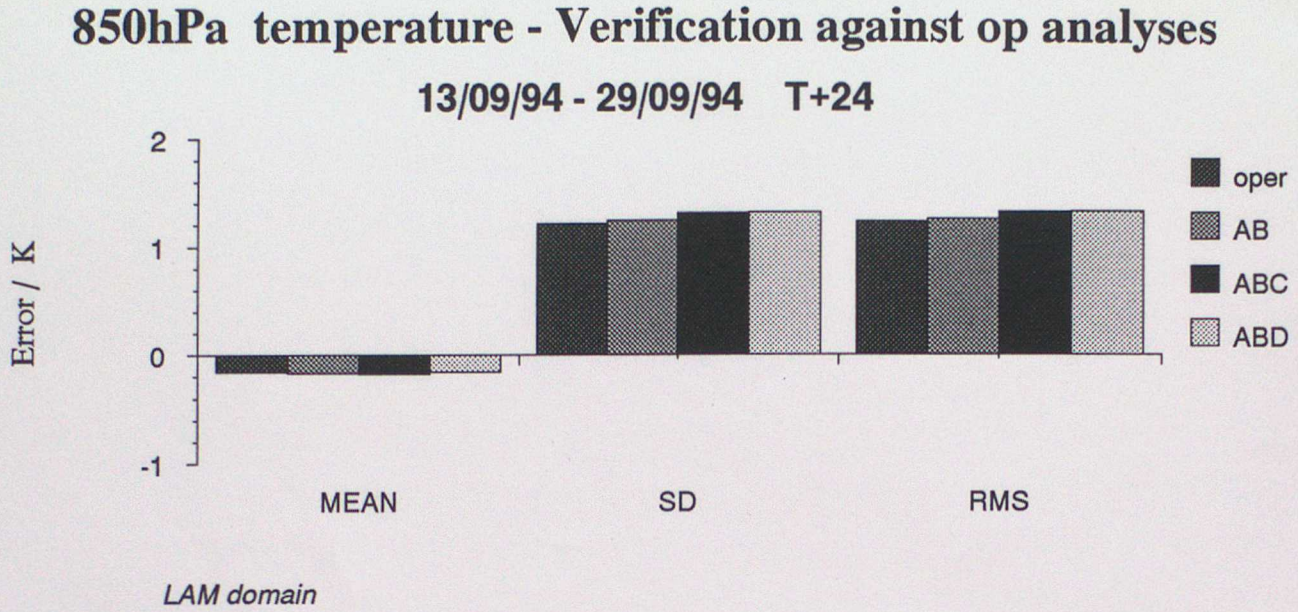

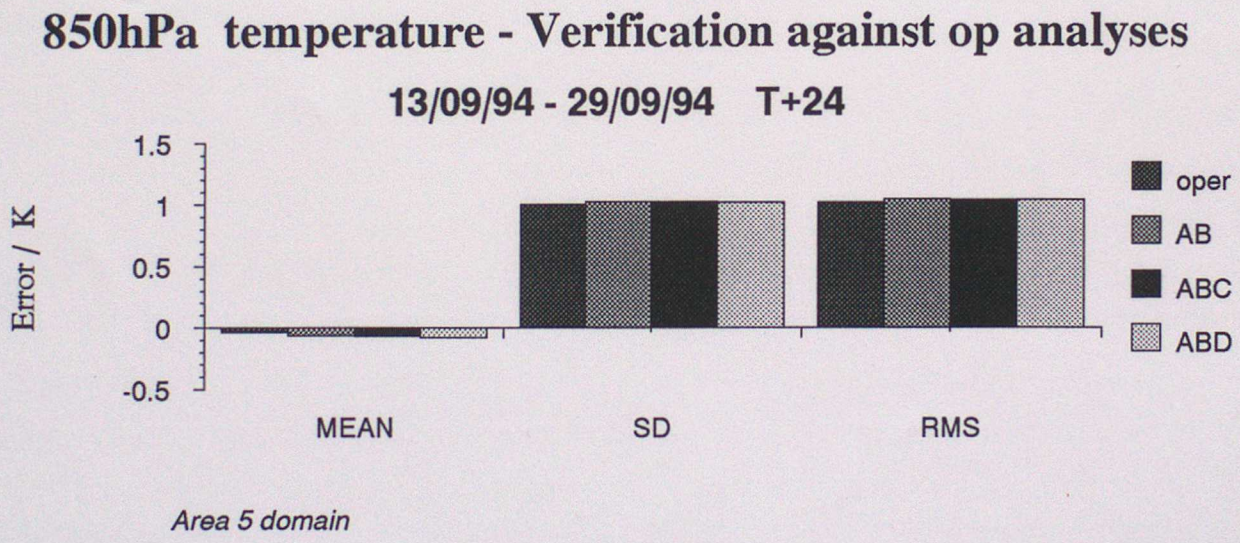

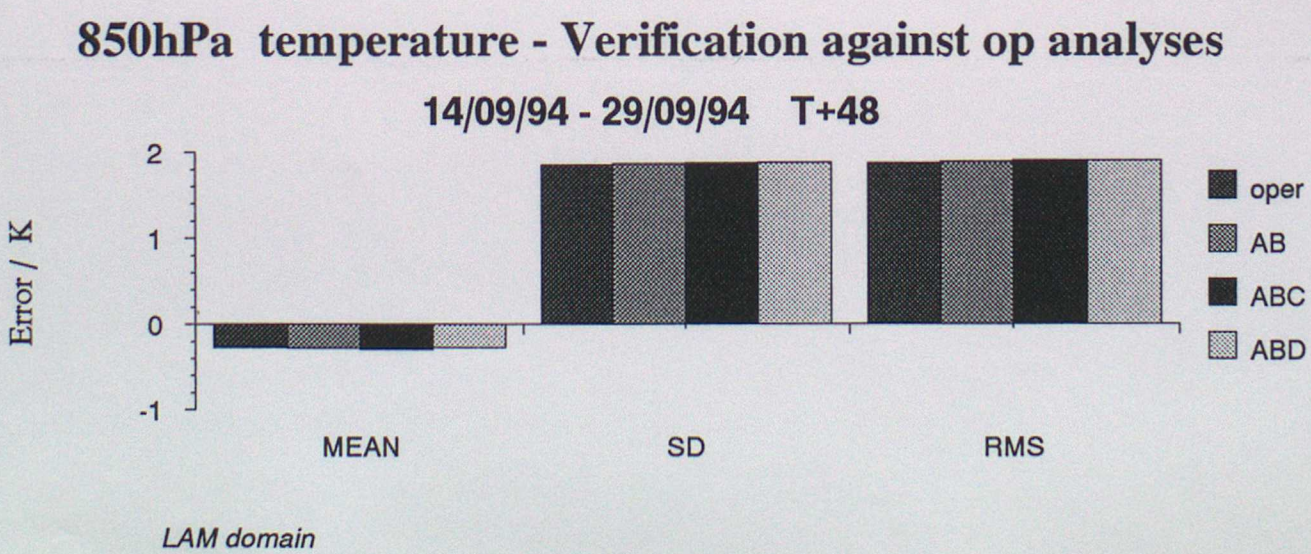

Figure 19 Verification of 850 hPa temperatures at T+24/48 against operational analyses

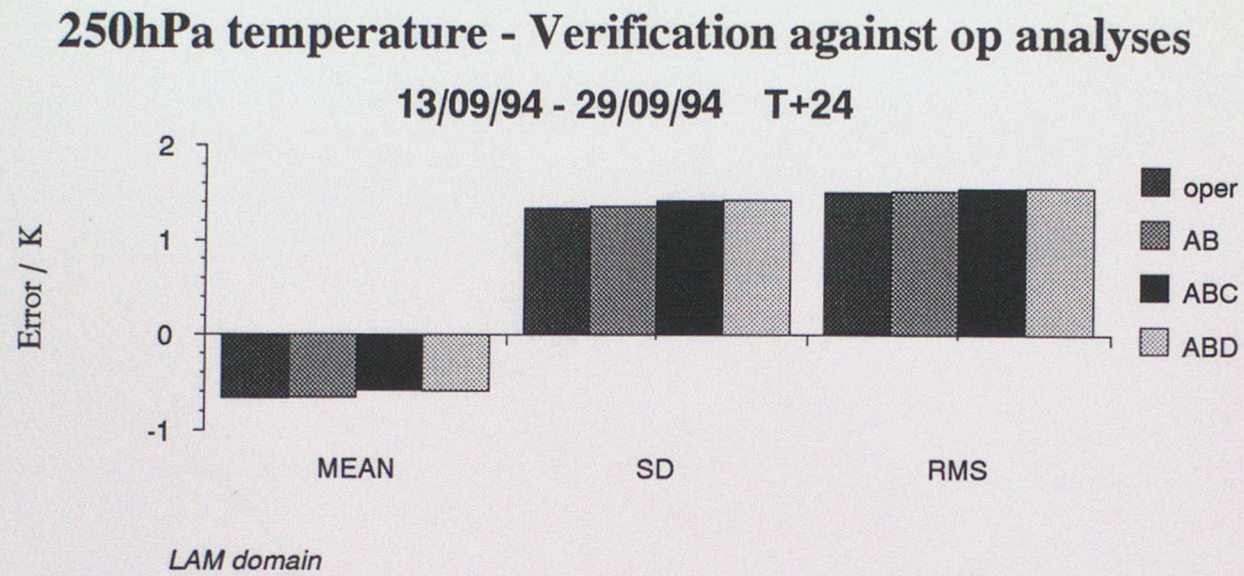

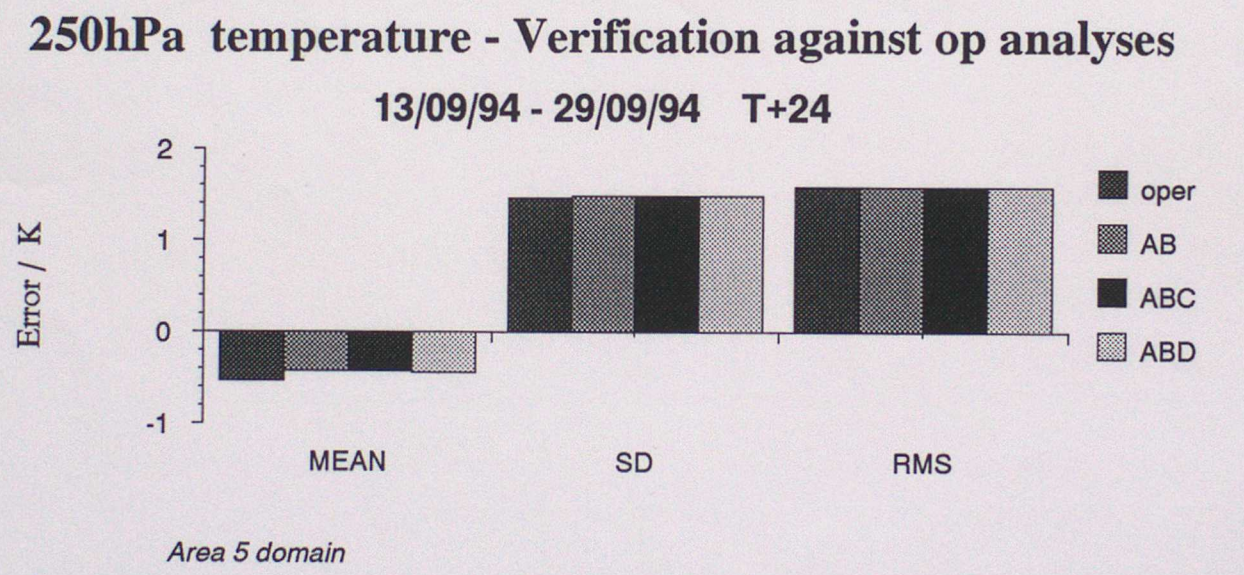

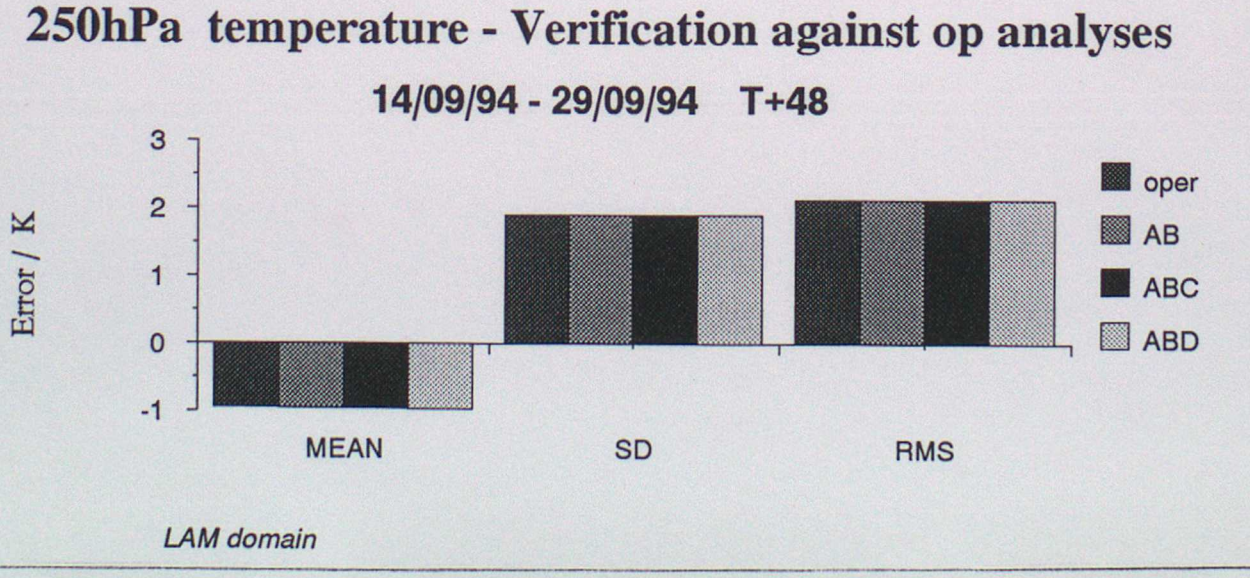

Figure 20 Verification of 250 hPa temperatures at T+24/48 against operational analyses.

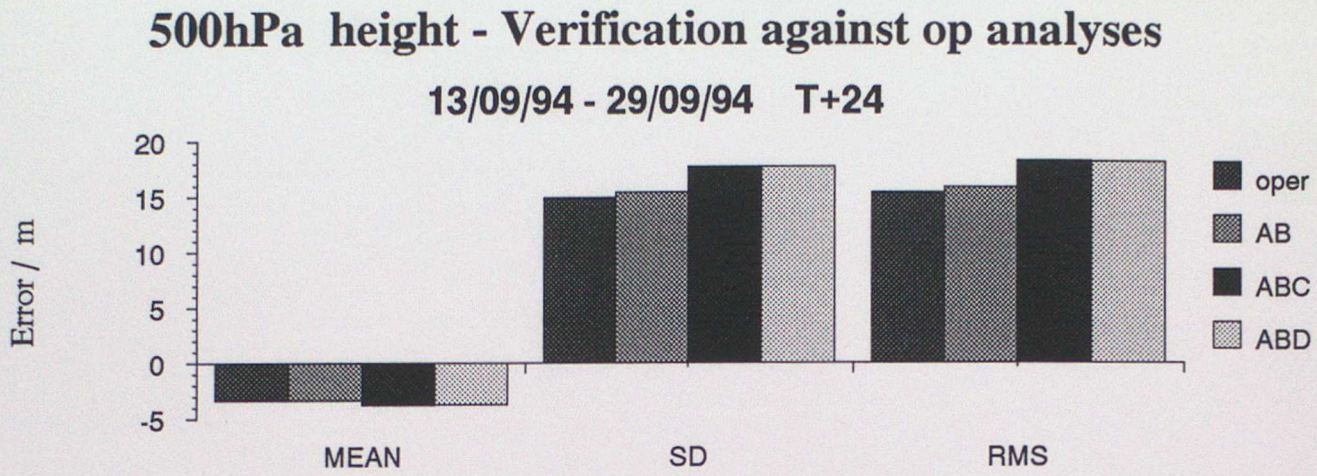

LAM domain

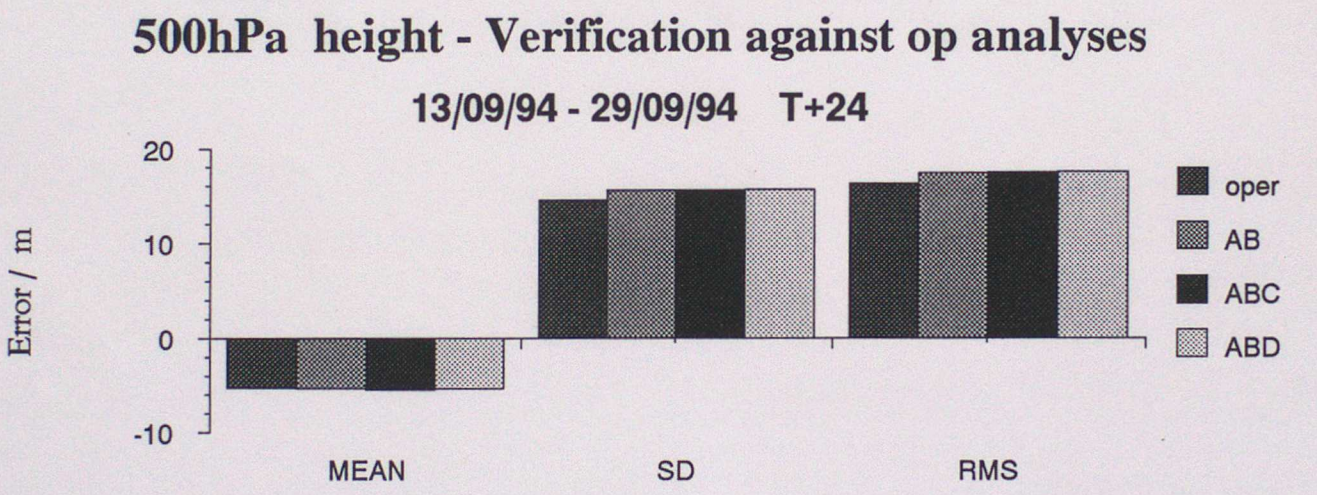

Area 5 domain

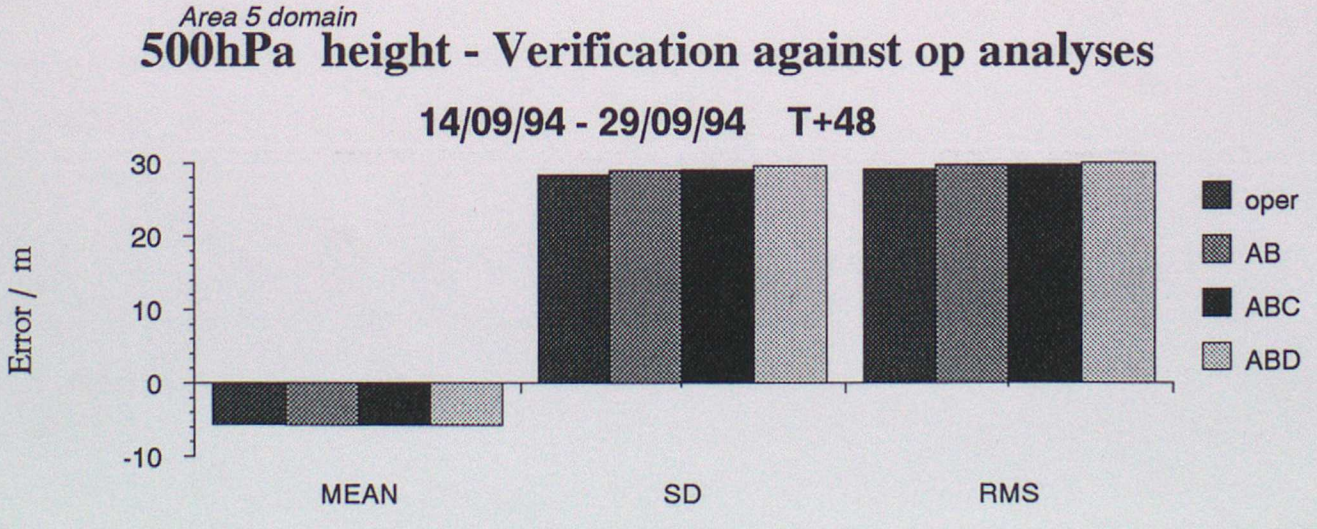

LAM domain

Figure 21 Verification of 500 hPa heights at T+24/48 against operational analyses.

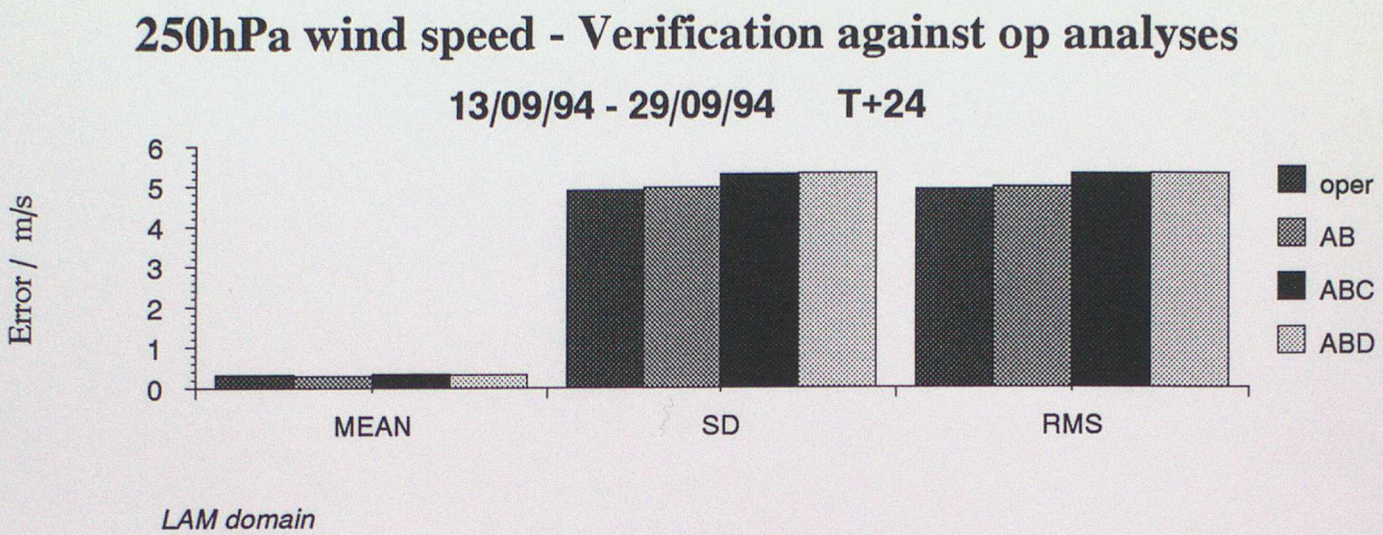

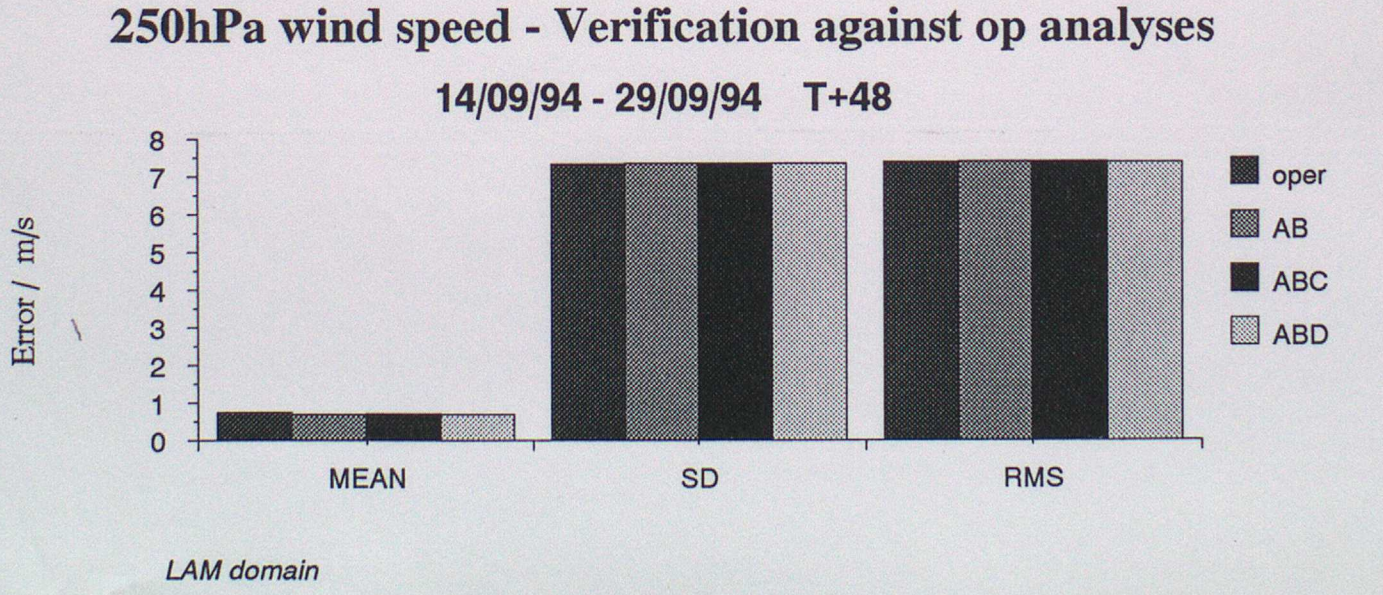

Figure 22 Verification of 250 hPa wind speed at T+24/48 against operational analyses.

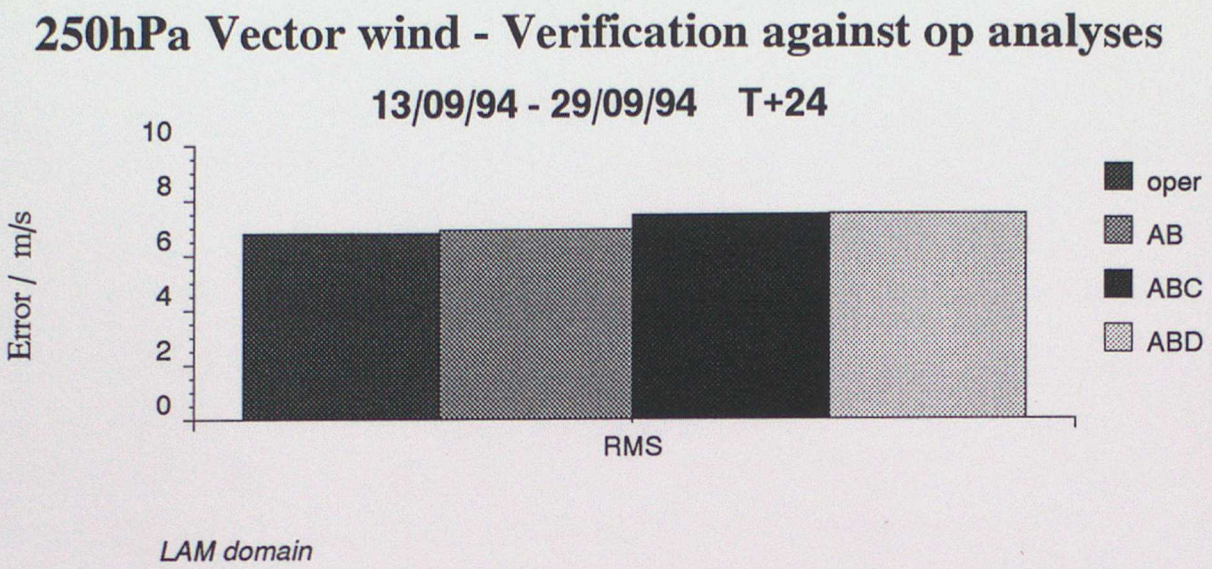

LAM domain

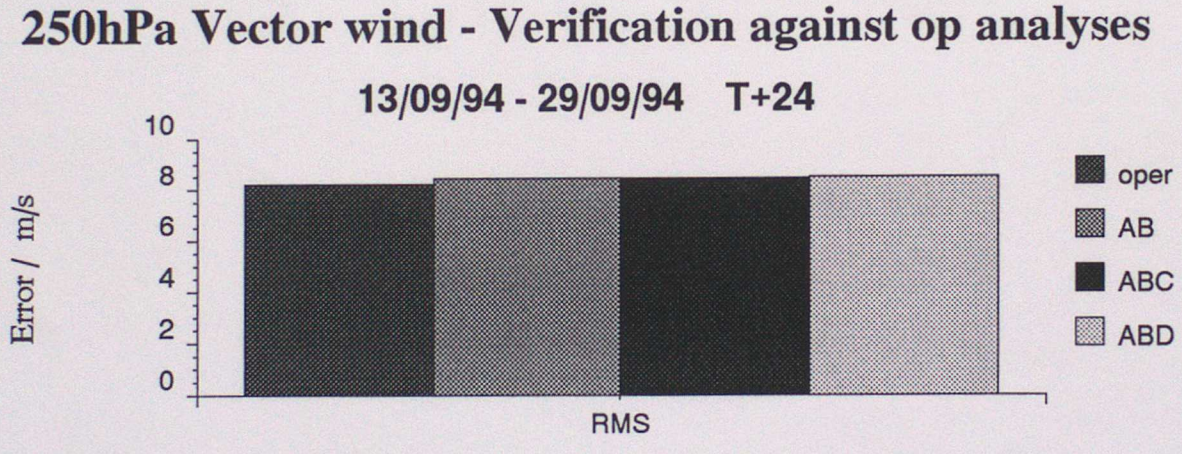

Area 5 domain

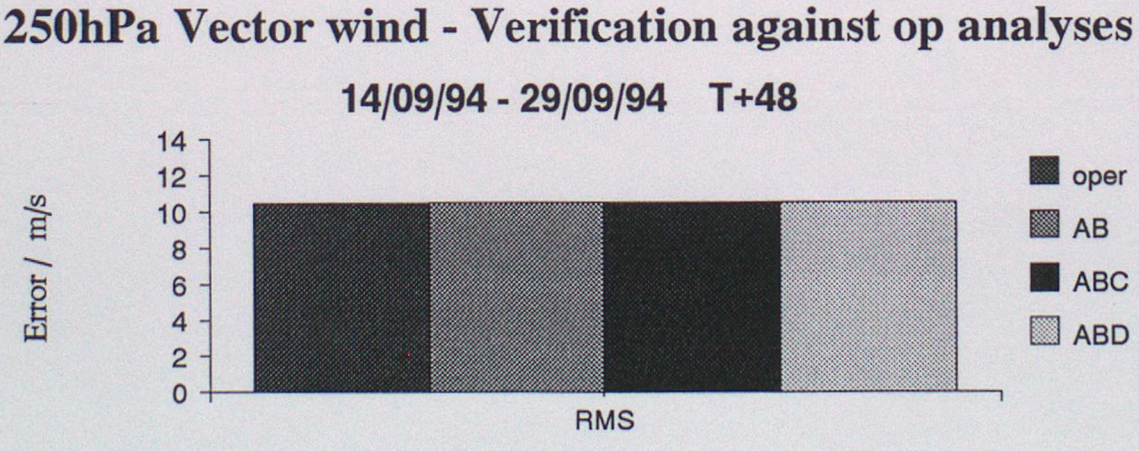

LAM domain

Figure 23 Verification of 250 hPa vector winds at T+24/48 against operational analyses.

Figure 24 Model level temperatures verified against sonde temperatures at T+72.

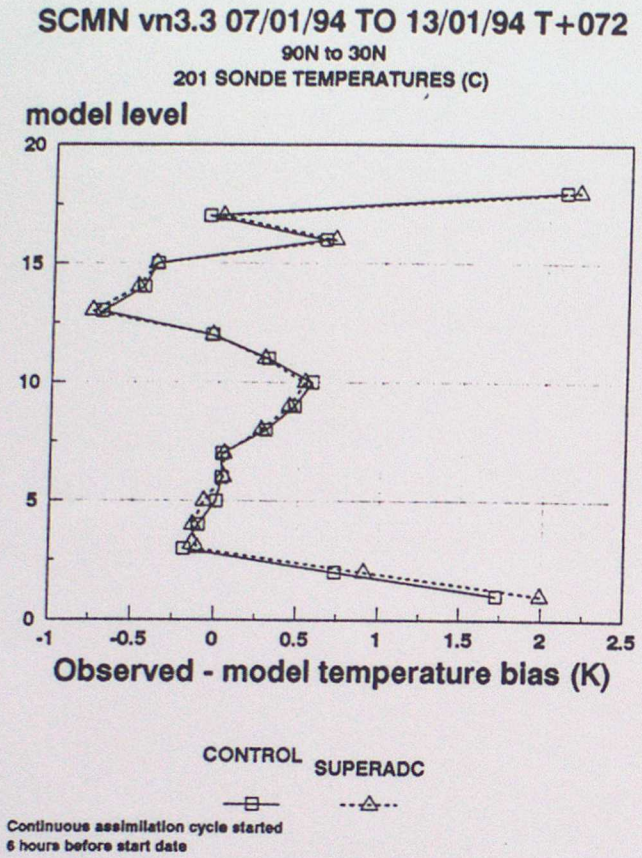

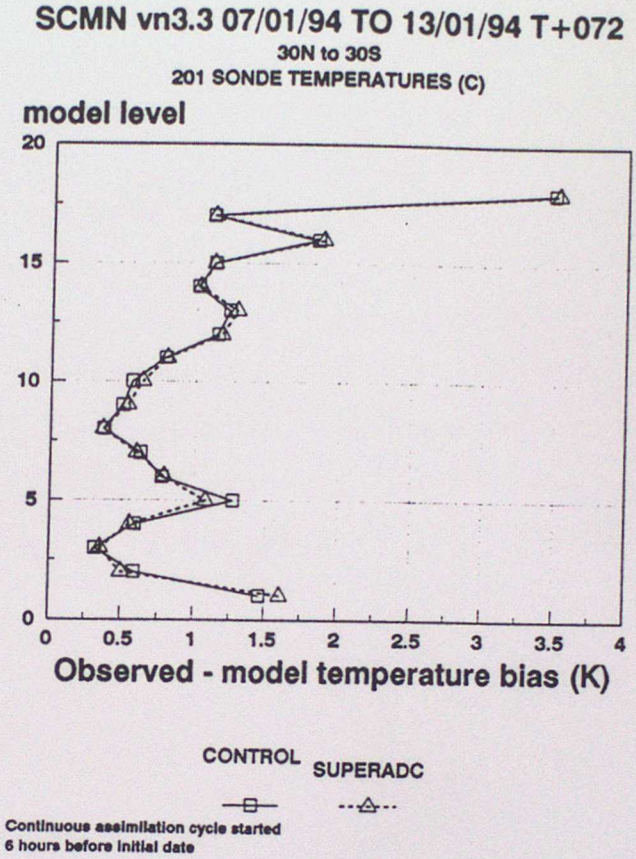

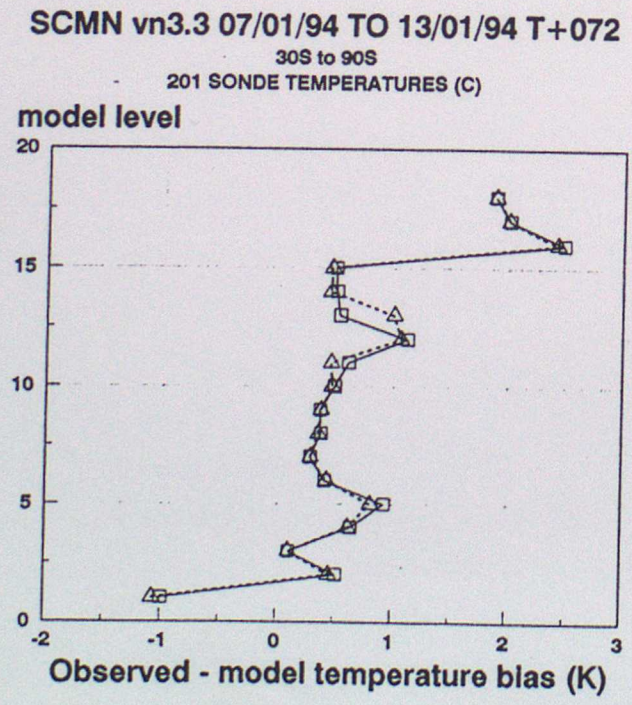

Figure 25 Model level temperatures verified against sonde temperatures at T+144.

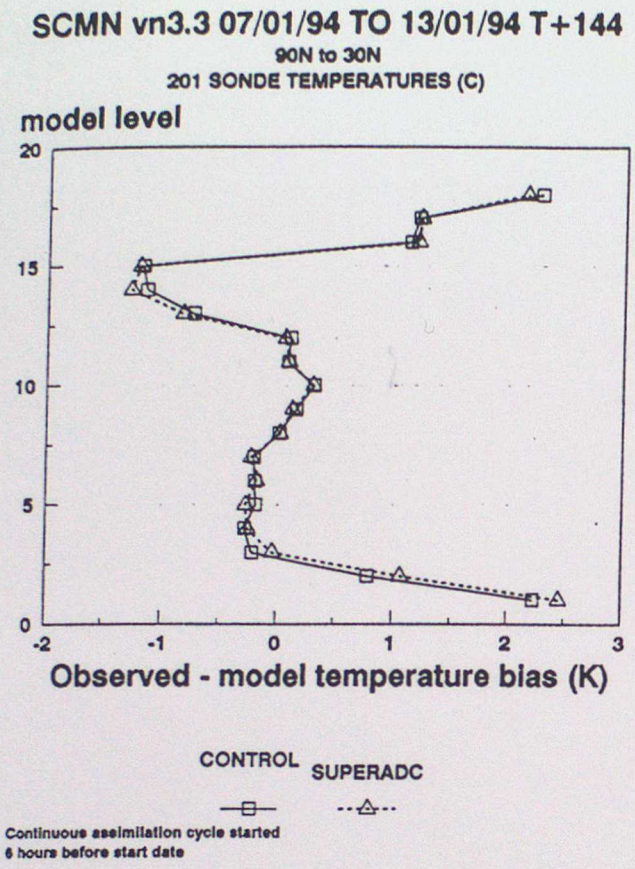

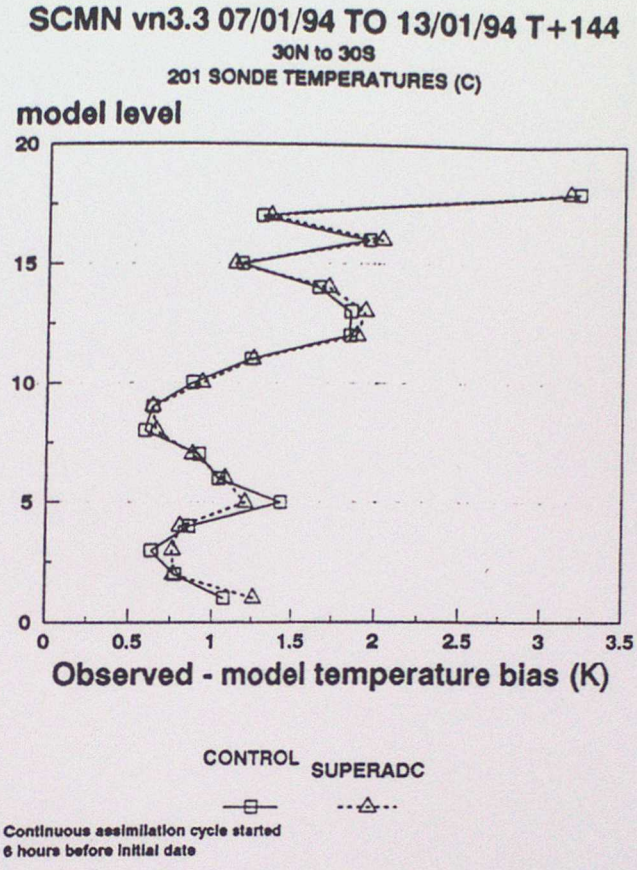

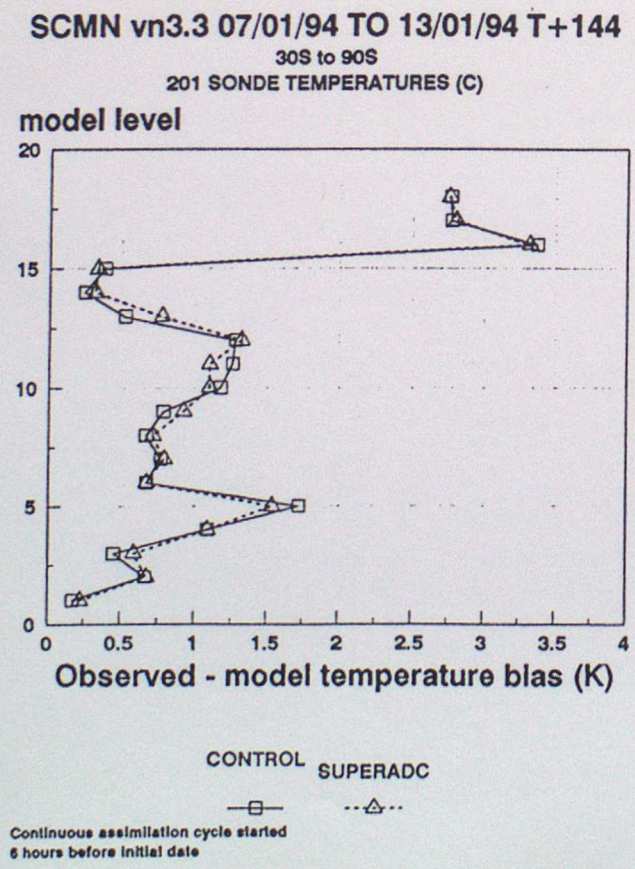

Figure 26 Model level relative humidities verified against sonde humidities at T+72.

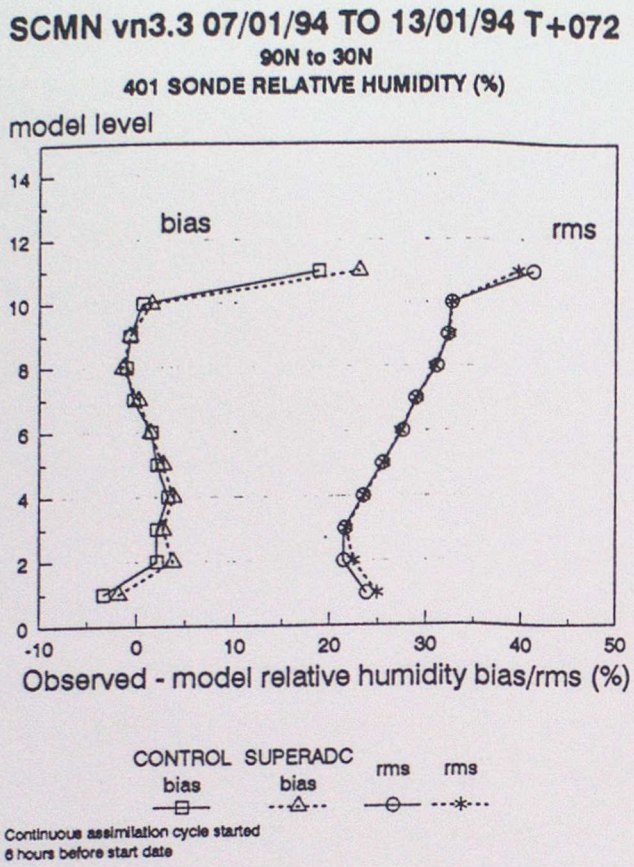

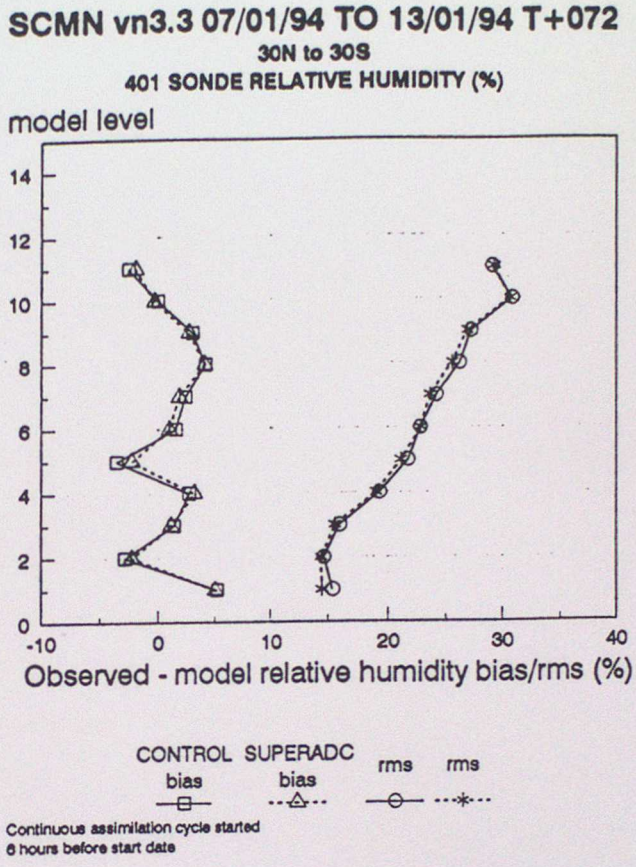

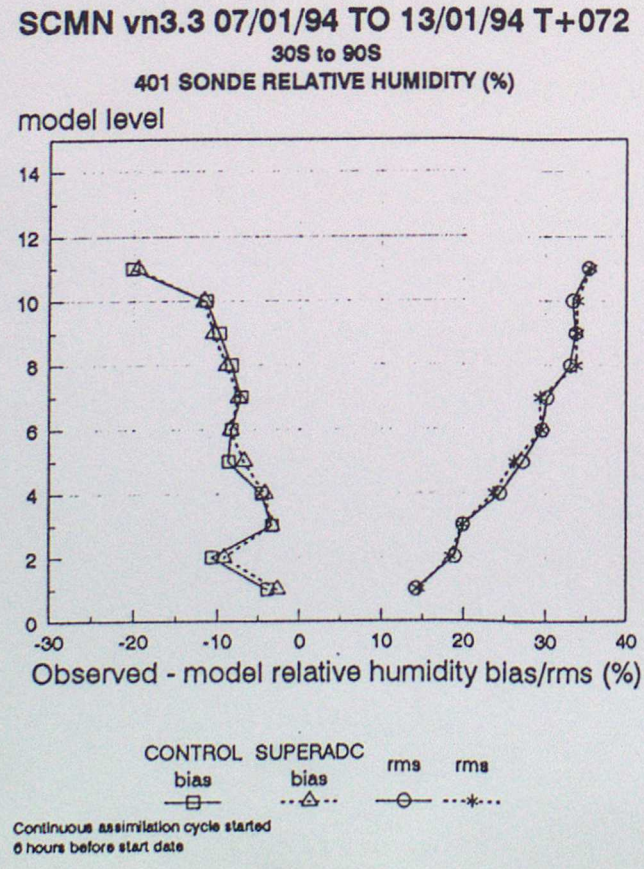

Figure 27 Model level relative humidities verified against sonde relative humidities at T+144.

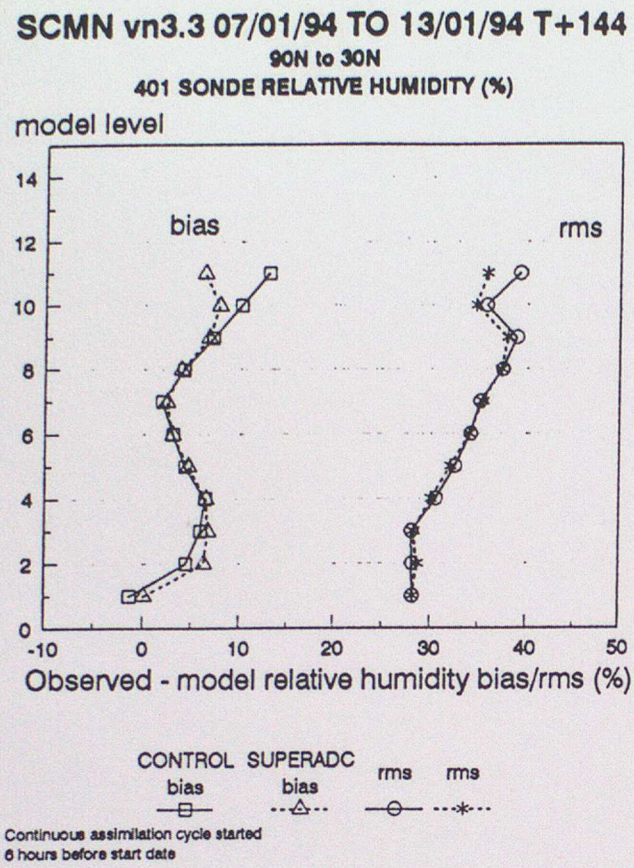

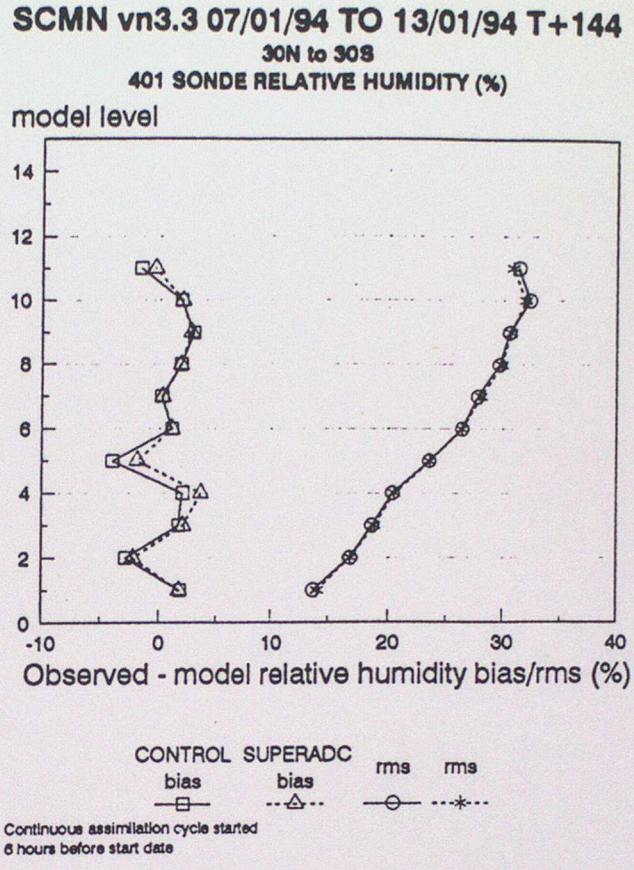

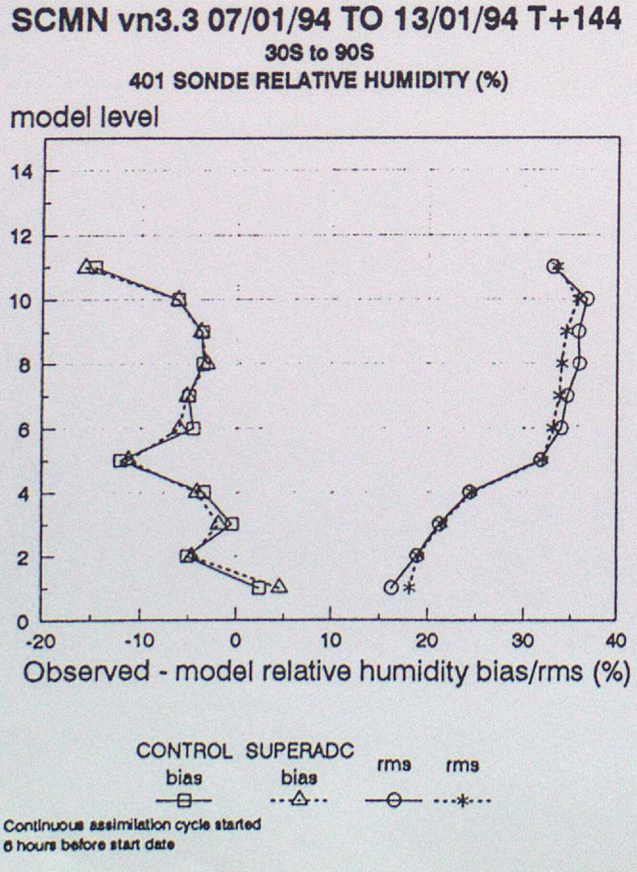

Figure 28 Model W wind bias errors against sonde winds at T+72.

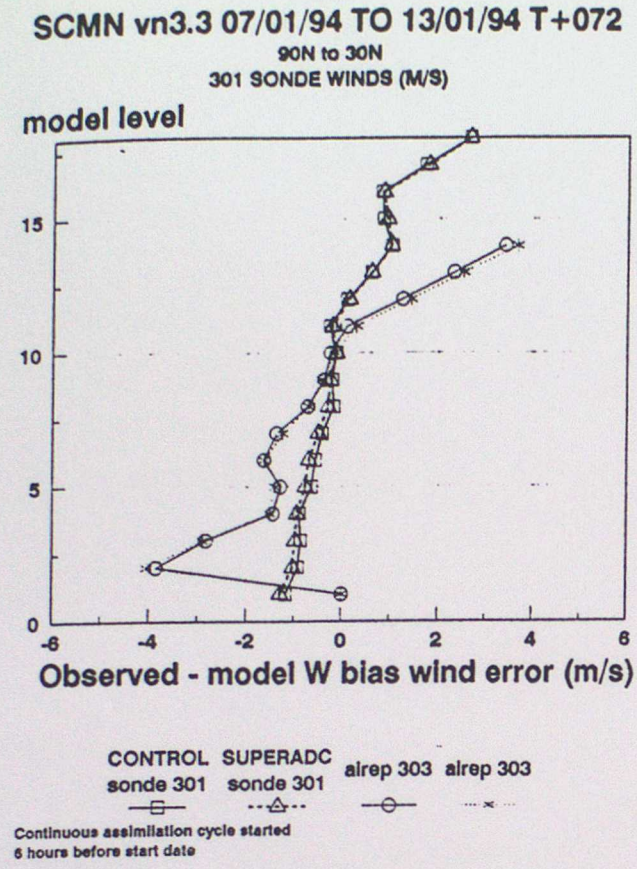

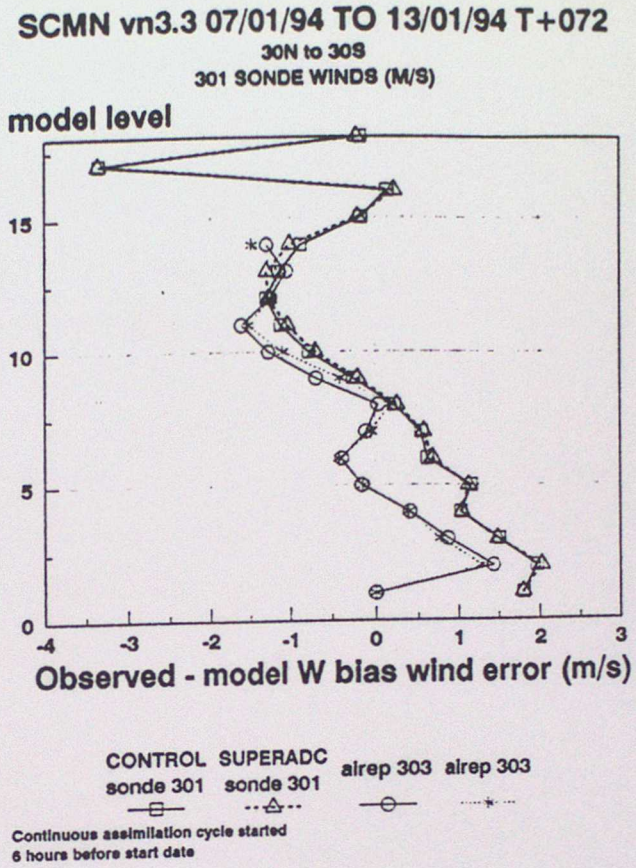

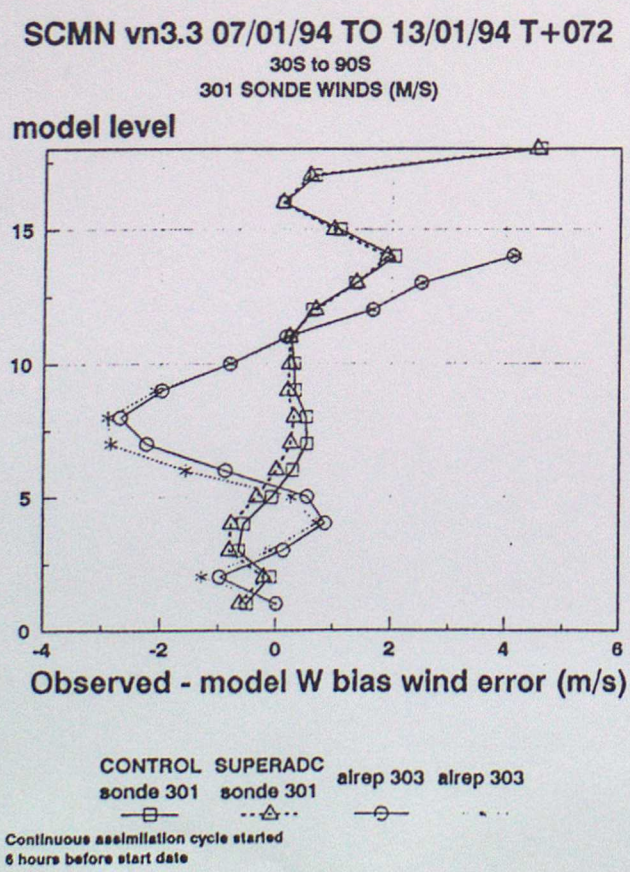

Figure 29 Model W wind bias errors against sonde winds at T+144.

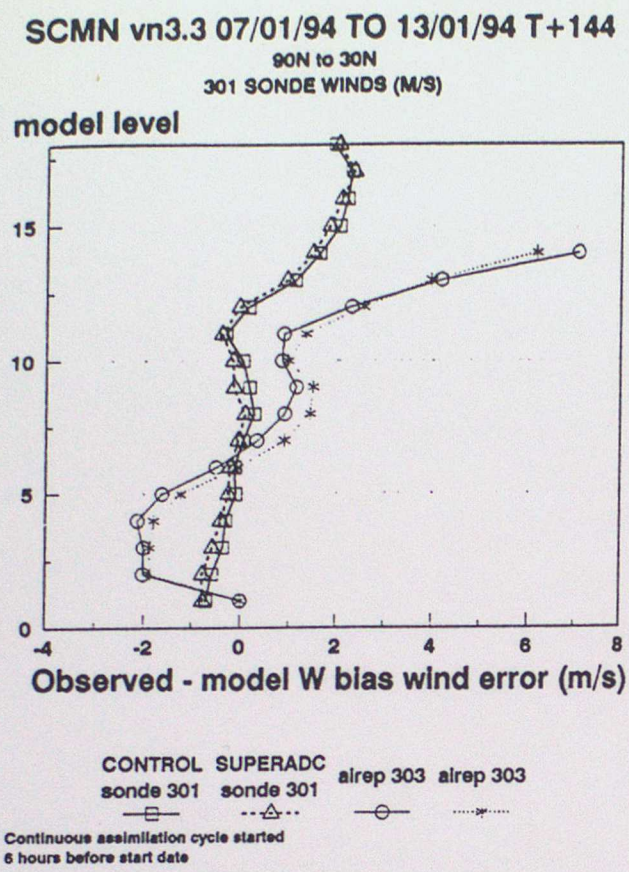

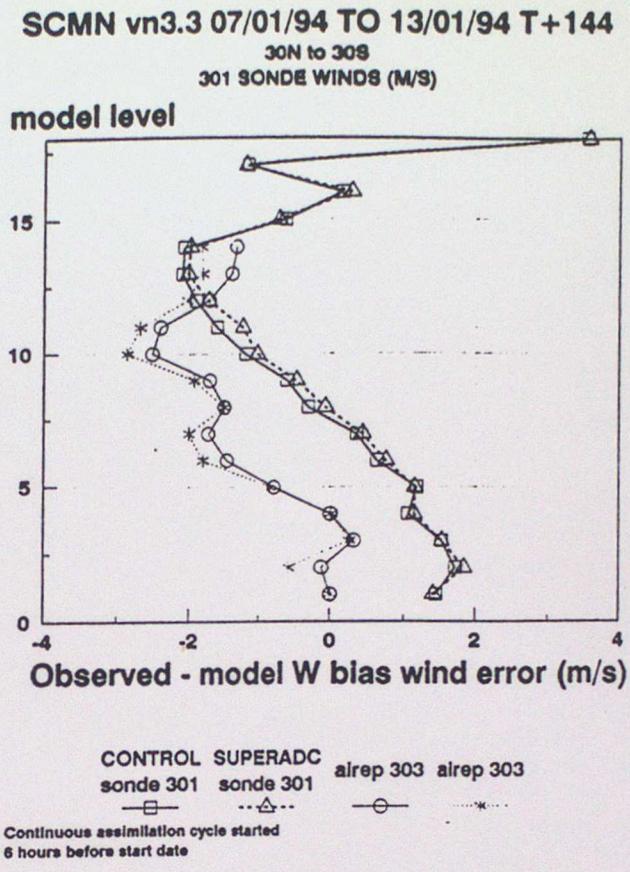

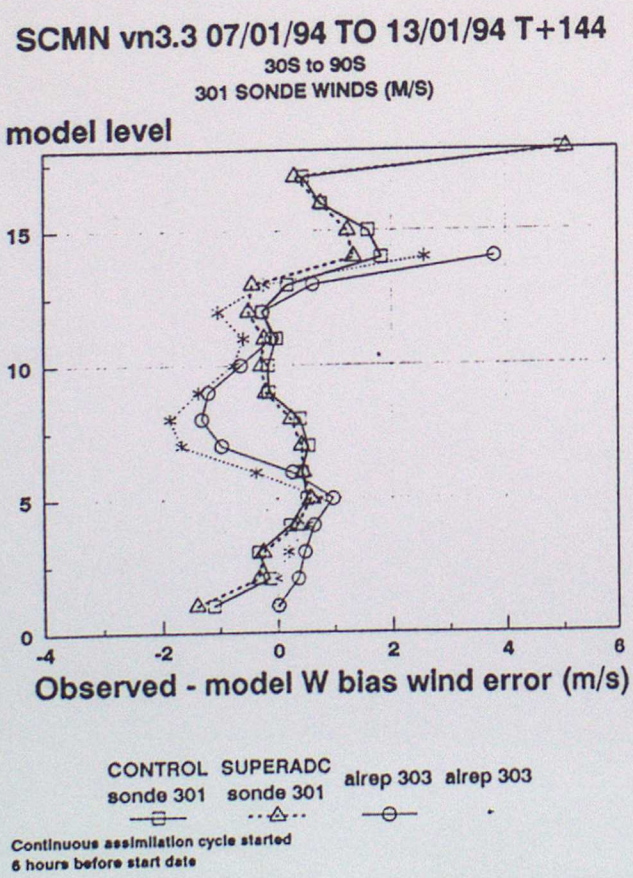

Figure 30 Model vector wind rms errors against sonde winds at T+72.

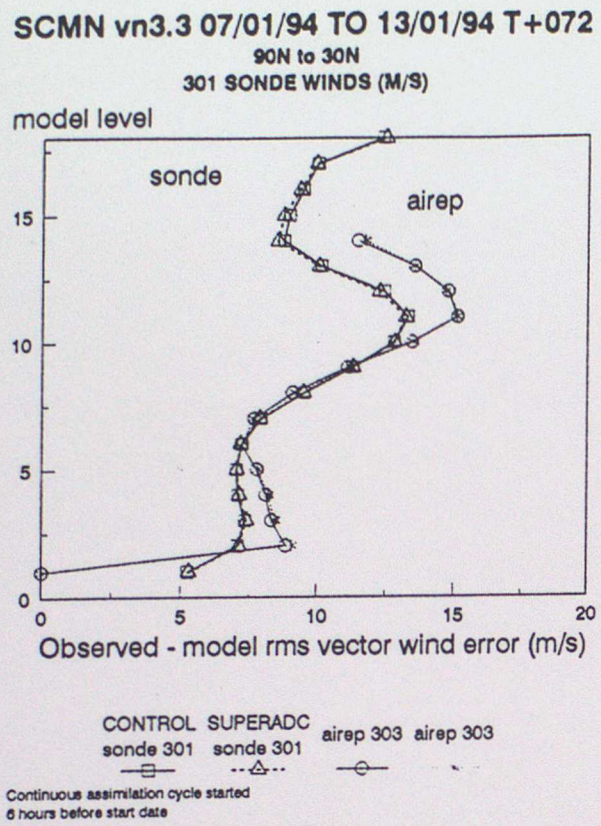

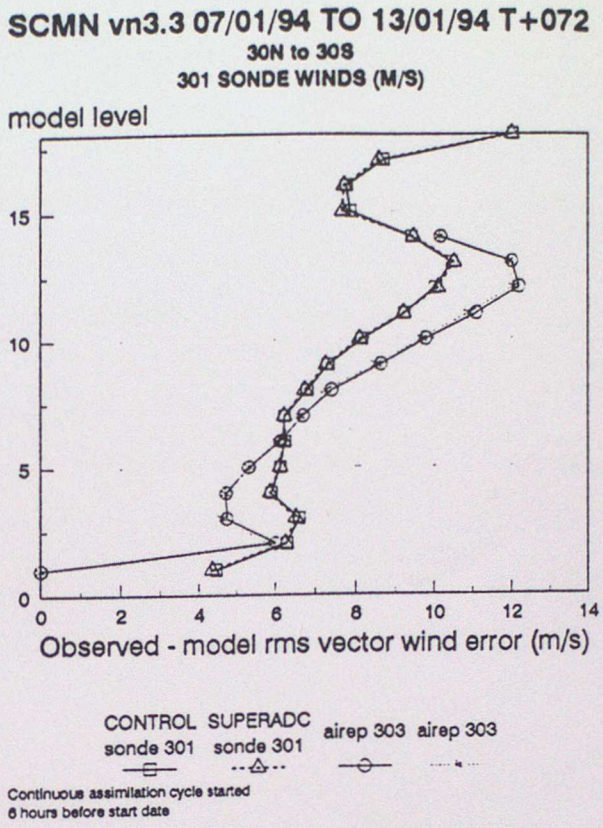

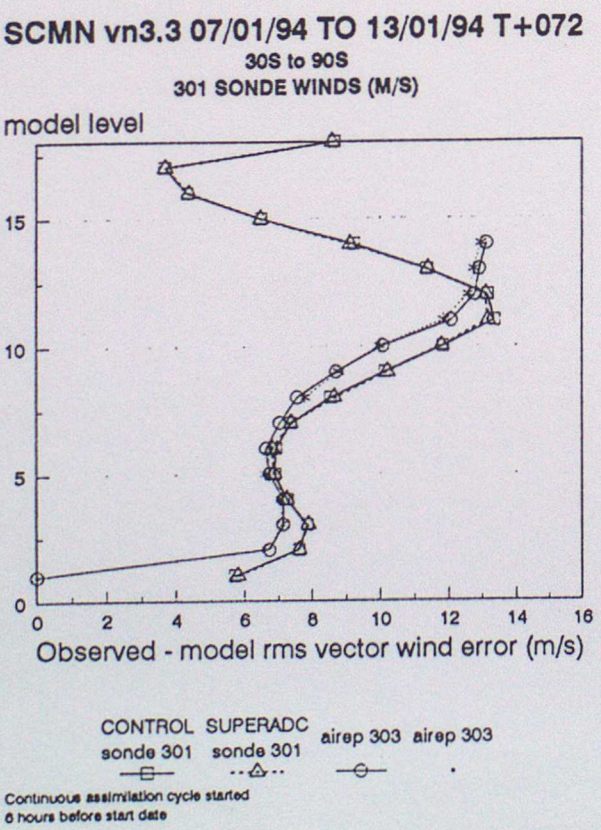
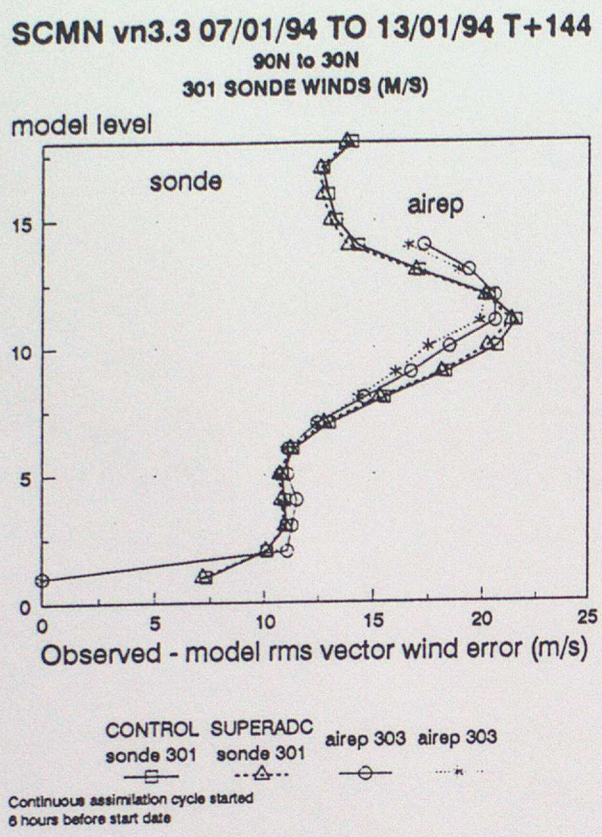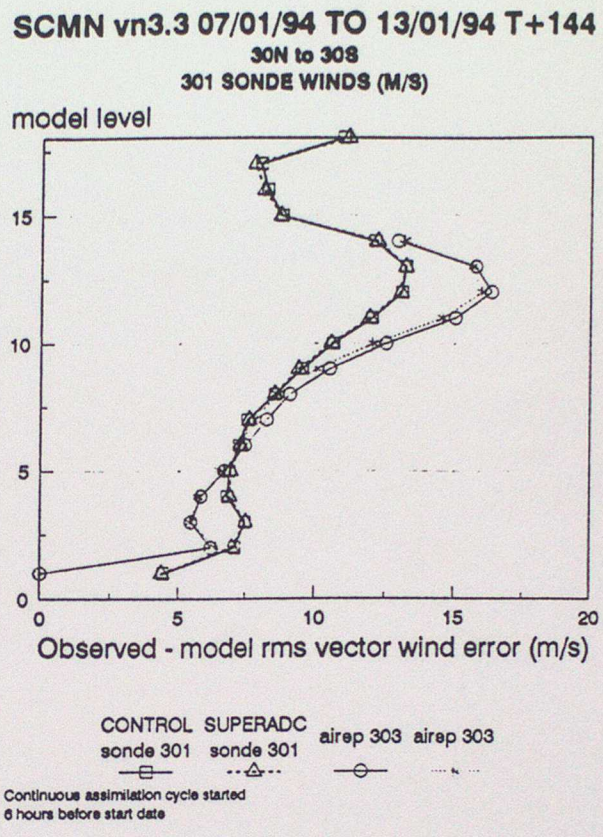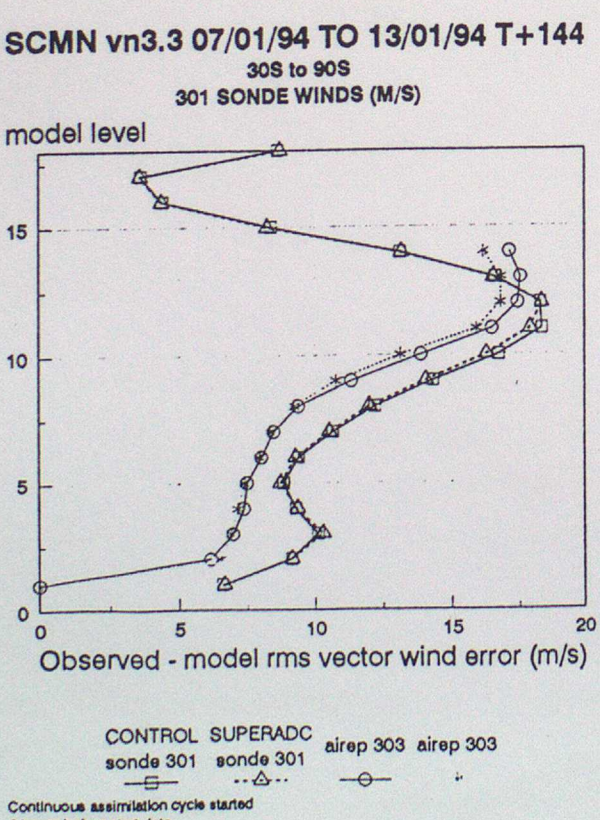
Figure 31 Model vector wind rms errors against sonde winds at T+144.